

# The protein kinase Sch9 is a key regulator of sphingolipid metabolism in *Saccharomyces cerevisiae*

Erwin Swinnen<sup>a,\*</sup>, Tobias Wilms<sup>a,\*</sup>, Jolanta Idkowiak-Baldys<sup>b</sup>, Bart Smets<sup>a</sup>, Pepijn De Snijder<sup>a</sup>, Sabina Accardo<sup>c</sup>, Ruben Ghillebert<sup>a</sup>, Karin Thevissen<sup>a,d</sup>, Bruno Cammue<sup>d</sup>, Dirk De Vos<sup>c</sup>, Jacek Bielawski<sup>b</sup>, Yusuf A. Hannun<sup>b</sup>, and Joris Winderickx<sup>a</sup>

<sup>a</sup>Functional Biology, <sup>c</sup>Centre for Surface Chemistry and Catalysis, and <sup>d</sup>Centre of Microbial and Plant Genetics, KU Leuven, 3001 Heverlee, Belgium; <sup>b</sup>Department of Biochemistry and Molecular Biology, Medical University of South Carolina, Charleston, SC 29403

**ABSTRACT** The *Saccharomyces cerevisiae* protein kinase Sch9 is an *in vitro* and *in vivo* effector of sphingolipid signaling. This study examines the link between Sch9 and sphingolipid metabolism in *S. cerevisiae* *in vivo* based on the observation that the *sch9Δ* mutant displays altered sensitivity to different inhibitors of sphingolipid metabolism, namely myriocin and aureobasidin A. Sphingolipid profiling indicates that *sch9Δ* cells have increased levels of long-chain bases and long-chain base-1 phosphates, decreased levels of several species of (phyto)ceramides, and altered ratios of complex sphingolipids. We show that the target of rapamycin complex 1–Sch9 signaling pathway functions to repress the expression of the ceramidase genes *YDC1* and *YPC1*, thereby revealing, for the first time in yeast, a nutrient-dependent transcriptional mechanism involved in the regulation of sphingolipid metabolism. In addition, we establish that Sch9 affects the activity of the inositol phosphosphingolipid phospholipase C, *Isc1*, which is required for ceramide production by hydrolysis of complex sphingolipids. Given that sphingolipid metabolites play a crucial role in the regulation of stress tolerance and longevity of yeast cells, our data provide a model in which Sch9 regulates the latter phenotypes by acting not only as an effector but also as a regulator of sphingolipid metabolism.

## Monitoring Editor

Benjamin S. Glick  
University of Chicago

Received: Jun 24, 2013

Revised: Oct 11, 2013

Accepted: Oct 29, 2013

## INTRODUCTION

Sphingolipids, together with sterols and glycerophospholipids, are essential components of all eukaryotic membranes. Much of the progress in the understanding of sphingolipid metabolism is due to research performed in the budding yeast *Saccharomyces cerevisiae*,

in which most, if not all, of the enzymes involved in sphingolipid metabolism have been identified (Figure 1; Funato *et al.*, 2002; Sims *et al.*, 2004; Dickson *et al.*, 2006). Apart from their structural function, sphingolipids also play important regulatory roles. More specifically, in yeast, sphingolipids are involved in the regulation of cellular processes as diverse as cell growth, endocytosis, actin cytoskeleton organization, protein trafficking, cell wall integrity, nutrient uptake, and longevity (Dickson, 2010). In these processes, signaling functions are ascribed not only to the complex sphingolipid species, but also to the intermediate metabolites, that is, the long-chain bases (LCBs), the long-chain base 1-phosphates (LCBPs), and ceramide species. Accumulating evidence in yeast and mammalian model systems strongly suggests that the dynamic balance between the different sphingolipid metabolites, often referred to as the LCB(P)/ceramide rheostat or sphingolipid rheostat, is an important factor determining their regulatory action (Kobayashi and Nagiec, 2003; Kihara *et al.*, 2007; Dickson, 2008; Matmati and Hannun, 2008; Breslow and Weissman, 2010; Bikman and Summers, 2011; Van Brocklyn and Williams, 2012). As such, proper regulation of this

This article was published online ahead of print in MBoC in Press (<http://www.molbiolcell.org/cgi/doi/10.1091/mbc.E13-06-0340>) on November 6, 2013.

\*These authors contributed equally to this work.

Address correspondence to: Erwin Swinnen ([erwin.swinnen@bio.kuleuven.be](mailto:erwin.swinnen@bio.kuleuven.be)), Joris Winderickx ([joris.winderickx@bio.kuleuven.be](mailto:joris.winderickx@bio.kuleuven.be)).

Abbreviations used: DHS, dihydrosphingosine; DHS-P, dihydrosphingosine-1-phosphate; IPC, inositolphosphoryl ceramide; LCB, long-chain base; LCBP, long-chain base 1-phosphate; MIPC, mannosylinositolphosphoryl ceramide; M(IP)2C, mannosyldiinositolphosphoryl ceramide; PHS, phytosphingosine; PHS-P, phytosphingosine-1-phosphate; ROS, reactive oxygen species; SPT, serine palmitoyl transferase; TORC, target of rapamycin complex; WT, wild type.

© 2014 Swinnen *et al.* This article is distributed by The American Society for Cell Biology under license from the author(s). Two months after publication it is available to the public under an Attribution–Noncommercial–Share Alike 3.0 Unported Creative Commons License (<http://creativecommons.org/licenses/by-nc-sa/3.0>).

“ASCB®,” “The American Society for Cell Biology®,” and “Molecular Biology of the Cell®” are registered trademarks of The American Society of Cell Biology.

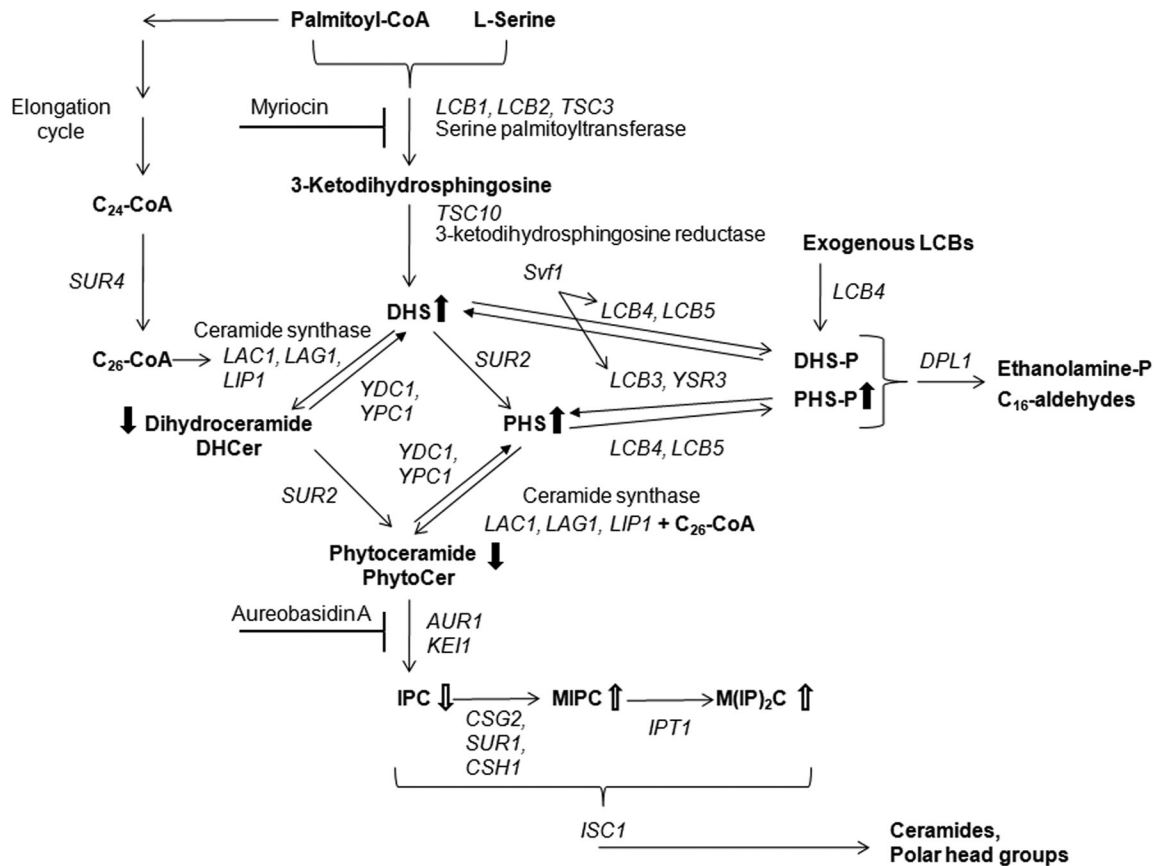


**FIGURE 1:** Schematic representation of sphingolipid biosynthesis (adapted from Dickson, 2008). A schematic representation of the de novo biosynthesis pathway for sphingolipids, with the genes encoding for the involved enzymes in *italic* and both the complex sphingolipids and the different intermediates of sphingolipid biosynthesis in **bold**. Used inhibitors of sphingolipid biosynthesis are shown. Changes in sphingolipid profile for the *sch9Δ* strain, compared with the WT strain, are indicated with closed arrows for LCB and ceramide species (see Figure 3 for results) and open arrows for complex sphingolipids (see Figure 7 for results).

balance is key to cellular survival, and recent reports have shed some light on the molecular mechanisms by which yeast controls this balance. For instance, the yeast Orm1 and Orm2 proteins are crucial regulators of sphingolipid homeostasis by controlling the activity of the serine palmitoyl transferase (SPT) enzyme, which catalyzes the first and rate-limiting step in de novo synthesis of sphingolipids. Orm1/2 are members of the conserved ORMDL family of endoplasmic reticulum (ER) membrane proteins (*ORMDL 1/2/3* genes in humans) and physically interact with SPT, inhibiting the activity of the enzyme (Breslow *et al.*, 2010; Han *et al.*, 2010). This inhibitory action is abrogated through Orm1/2 phosphorylation by the protein kinase Ypk1 (Roelants *et al.*, 2011). When sphingolipid levels drop—for example, when cells are treated with the SPT inhibitor myriocin—the target of rapamycin complex 2 (TORC2) kinase activates Ypk1, boosting de novo sphingolipid synthesis to counteract dropping sphingolipid levels. In addition, the increase in LCB accumulation on heat shock is also dependent on Ypk1's action, downstream of the Pkh1/2 kinases (Sun *et al.*, 2012).

Interestingly, as yeast cells approach stationary phase, they accumulate LCBs and LCBPs as well (Lester *et al.*, 2013). This increase may also be mediated in part by an increase in SPT activity, although additional mechanisms, such as a decrease in ceramide synthase activity as cells enter the stationary phase, were also demonstrated. Although phosphorylation of the Orm proteins depends on the

rapamycin-sensitive, nutrient-responsive TORC1 kinase, recent evidence shows that these phosphorylation sites are distinct from those regulated by myriocin treatment, indicating that TORC1 and TORC2 have distinct roles in the control of the Orm proteins (Liu *et al.*, 2012; Shimobayashi *et al.*, 2013). Indeed, rapamycin-induced phosphorylation of Orm1/2 did not seem to affect SPT activity. Instead, a stimulation of complex sphingolipid synthesis was observed, through as-yet-unknown mechanisms. Additional evidence for a nutrient-dependent regulation of complex sphingolipid levels comes from a recent lipidomic approach, in which it was shown that relative levels of different complex sphingolipid species change as yeast cells enter the stationary phase (Klose *et al.*, 2012).

To help coordinate cellular responses to changing nutrient levels, yeast depends on Sch9, a protein kinase with a central role in the carbon and nitrogen source-dependent signaling pathway that controls cell growth, longevity, and stress resistance (Toda *et al.*, 1988; Crauwels *et al.*, 1997; Fabrizio *et al.*, 2001; Roosen *et al.*, 2005; Smets *et al.*, 2008, 2010). Sch9 performs this function, in part, by acting as an effector of the TORC1 complex (Urban *et al.*, 2007), although several studies indicated that Sch9 also acts independently of TORC1 (Yorimitsu *et al.*, 2007; Smets *et al.*, 2008). Like Ypk1/2, Sch9 can be phosphorylated by Pkh1 and Pkh2 at its PDK1 site in its activation loop, and this phosphorylation is indispensable for its function (Roelants *et al.*, 2004; Urban *et al.*, 2007; Voordeckers *et al.*,

2011). In line with the suggested activation of Pkh1/2 by the long-chain base phytosphingosine (PHS), the phosphorylation and activation of Sch9 by Pkh1 is enhanced *in vitro* by the addition of PHS (Liu *et al.*, 2005) and lowered *in vivo* by pharmacological or genetic reduction of sphingolipid synthesis (Huang *et al.*, 2012; Liu *et al.*, 2013). Hence these results indicate that Sch9 is an effector of sphingolipid signaling.

In this study, we examine the link between Sch9 and sphingolipid metabolism in more detail. Our data demonstrate that Sch9 has a regulatory role in *de novo* ceramide biosynthesis and ceramide production by hydrolysis of complex sphingolipids. We provide evidence for a transcriptional regulatory mechanism in which Sch9 is required to repress ceramidase activity during growth by acting downstream of the TORC1 kinase. In addition, for hydrolytic ceramide production, Sch9 is essential for the proper translocation of the inositol phosphosphingolipid phospholipase C, *Isc1*, from the ER to mitochondria during the diauxic shift. As such, Sch9 appears to be the gatekeeper of a monitoring system required to balance biosynthetic and hydrolytic ceramide production. We illustrate and discuss some of the phenotypic repercussions associated with this role of Sch9, focusing on mitochondrial activity, oxidative stress, aging, and longevity. Given the function of Sch9 in nutrient signaling and the fact that sphingolipids mediate Pkh-dependent phosphorylation and activation of Sch9, one obvious conclusion is that Sch9 is part of a feedback system balancing the sphingolipid rheostat in response to both internal sphingolipid signals and nutrient availability.

## RESULTS

### Deletion of *SCH9* confers resistance to myriocin and increases sensitivity to aureobasidin A and phytosphingosine

To investigate the potential relationship between Sch9 and sphingolipid mediated signaling, we compared myriocin resistance of wild-type (WT) cells and isogenic *sch9Δ* mutants. Myriocin is an inhibitor of serine palmitoyl transferase (Figure 1), the primary enzyme in sphingolipid biosynthesis, encoded by *LCB1*, *LCB2*, and *TSC3* (Miyake *et al.*, 1995; Sun *et al.*, 2000). The analysis was performed in two genetic backgrounds, W303-1A and BY4741, to ensure that the observed effects were not related to the background used. The analysis also compared the use of different selection markers to create the deletion of *SCH9* in order to exclude possible marker effects. In all cases we found that cells lacking Sch9 displayed an increased myriocin resistance, as visualized by spot assays (Figure 2A). Overexpression of *SCH9* in the *sch9Δ* mutant restored myriocin sensitivity (Figure 2B), indicating that the presence or absence of a functional Sch9 is the only factor that contributes to the observed differences in myriocin resistance. To evaluate whether increased myriocin resistance reflects increased survival, we performed a propidium iodide (PI) staining on WT cells and *sch9Δ* cells treated with 0.5 μg/ml myriocin. As shown in Figure 2C, the viability of *sch9Δ* cells was hardly affected by myriocin treatment ( $0.7 \pm 0.3\%$  dead cells), whereas that of WT cells was markedly decreased ( $23.8 \pm 3.4\%$  dead cells). Next we examined the effect of myriocin on the expression of ribosomal protein genes. Expression of these genes is tightly coupled to growth conditions, as they are induced under favorable conditions but repressed under adverse conditions. As expected, myriocin treatment triggered a significant decrease of ribosomal protein gene expression in WT cells, but had no effect in *sch9Δ* cells (Figure 2D).

We then investigated the sensitivity of WT and *sch9Δ* cells to PHS. Maintaining the balance in intermediary sphingolipid metabolites is of utmost importance for cell growth and survival. Addition

of low concentrations of PHS rescues myriocin toxicity (Sun *et al.*, 2000), whereas addition of high concentrations of PHS inhibits cell growth (Ella *et al.*, 1997; Skrzypek *et al.*, 1998; Chung *et al.*, 2001). Analysis of the growth of *sch9Δ* mutant and WT cells in the presence of different concentrations of PHS revealed that *sch9Δ* mutant cells are more sensitive to the growth-inhibitory effect of PHS than WT cells (Figure 2E), suggesting that cells lacking Sch9 already have higher internal pools of LCBs and LCBPs. In line with this are the data obtained upon monitoring the effect of the fungicide aureobasidin A. This fungicide inhibits Aur1 (Figure 1), an enzyme responsible for the production of the complex sphingolipid inositolphosphoryl ceramide (IPC; Heidler and Radding, 1995). The toxicity of aureobasidin A is due not only to the inhibition of the synthesis of complex sphingolipids, but also to the accumulation of LCBs (Nagiec *et al.*, 1997). Consistently, we observed that the *sch9Δ* mutant was more sensitive to aureobasidin A than the WT strain (Figure 2F).

### Deletion of *SCH9* alters the LCB(P)/ceramide balance

To evaluate the hypothesis that cells lacking Sch9 have higher levels of intermediary sphingolipid metabolites and thus that Sch9 may function as modulator of sphingolipid metabolism *in vivo*, we determined the levels of PHS and dihydrosphingosine (DHS), their phosphates, phytosphingosine-1-phosphate (PHS-P) and dihydrosphingosine-1-phosphate (DHS-P), and the levels of (phyto)ceramides in the membranes of the WT and the *sch9Δ* strain. Compared to the WT strain, *sch9Δ* cells were characterized by increased levels of DHS, PHS, and PHS-P, whereas levels of DHS-P remained below the detection limit (Figure 3A). Conversely, the concentrations of the ceramides C<sub>18</sub>-dihydroceramide, C<sub>20</sub>-dihydroceramide, and C<sub>26</sub>-phytoceramide were decreased in *sch9Δ* cells (Figure 3, B and C), as was the amount of α-hydroxylated phytoceramide (αOH-PhytoCer-C<sub>26</sub>; Figure 3D). Thus, these data suggest that the Sch9 protein kinase fulfills a regulatory role to maintain *de novo* ceramide synthesis.

An increase of LCB(P)s in *sch9Δ* cells could be the result of an increase in SPT activity, perhaps through phosphorylation of the Orm proteins. However, in this case we would expect that also ceramide levels would have increased, as shown before for the *orm1Δ orm2Δ* strain (Breslow *et al.*, 2010; Shimobayashi *et al.*, 2013). Alternatively, Sch9 could also be involved in very long-chain fatty acid formation, which serves as a substrate in the ceramide production (Figure 1). As such, the LCB(P)s may accumulate due to the inability to react with very long-chain fatty acids to form ceramides, as is the case in *sur4Δ* cells (Breslow *et al.*, 2010). However, we present genetic evidence that *SCH9* and *SUR4* work in parallel pathways, making this possibility unlikely (Supplemental Figure S1, B and C). Therefore a more obvious explanation is that Sch9 plays a role at the step of ceramide production or breakdown. This is supported by our genetic data showing that deletion of either gene encoding ceramidase (*YDC1* or *YPC1*) abrogates myriocin resistance of the *sch9Δ* strain (Supplemental Figure S1A), as does overexpression of the ceramide synthase *LAG1* or *LAC1* (Supplemental Figure S1D). To have a closer look at the enzymes involved in ceramide production and breakdown, we constructed WT and *sch9Δ* strains expressing chromosomally encoded, Myc-tagged versions of *Lag1*, *Lac1*, *Ydc1*, and *Ypc1* and analyzed their protein levels. We included the addition of rapamycin in these experiments, as this compound is well known for its ability to inactivate TORC1, a major nutrient-dependent activator of Sch9 (Urban *et al.*, 2007). Results in Figure 4 indicate that either deleting *SCH9* or treating WT cells with rapamycin increases the presence of the ceramidases *Ydc1* and *Ypc1*.

Because this effect of rapamycin addition is abrogated in *sch9Δ* cells, this suggests that Sch9 functions to repress ceramidase levels downstream of TORC1. Concerning the levels of the ceramide synthases, we also observed an increase in the levels of Lag1 and Lac1 in the *sch9Δ* strain, although the effects on Lac1 were not statistically significant. Of importance, this increase in Lag1/Lac1 levels is not seen when treating WT or *sch9Δ* cells with rapamycin. One possible explanation is that Sch9 might specifically regulate ceramide synthase levels, independent of TORC1. Note, however, that the rapamycin treatment represents a short-term response to TORC1 inactivation, whereas conditions for the *sch9Δ* strain represent a steady state of this strain during growth. Therefore, an alternative explanation is that during steady-state growth under nutrient-rich conditions, the increased abundance of ceramidase enzymes in the *sch9Δ* strain may trigger additional (TORC1-independent) homeostatic mechanisms, which increase Lag1/Lac1 levels to try to compensate the imbalanced sphingolipid rheostat. Because elevated levels of phosphorylated LCBs act as inhibitory to growth (Kim et al., 2000), this compensatory response could function to reduce LCB(P) levels to some extent to avoid complete growth inhibition.

### Sch9 controls de novo ceramide synthesis via transcriptional regulation mechanisms

To investigate whether the changes in protein levels under our experimental conditions reflect a transcriptional response, we constructed lacZ reporter fusions with the promoters of *LAG1*, *LAC1*, *YDC1*, and *YPC1* in the multicopy plasmid Yep357. First, Figure 5A shows that deletion of *SCH9* indeed results in a significant induction in reporter activity for both the ceramide synthase promoters, *LAG1* and *LAC1*, as for the ceramidase promoters *YDC1* and *YPC1*. This induction in the *sch9Δ* strain was higher for the ceramidase promoters compared with the induction of the promoters of the ceramide synthase genes, and as such correlates with our observation that the increase in protein levels for Ydc1-Myc and Ypc1-Myc is larger than the increases in Lag1-Myc and Lac1-Myc levels in the *sch9Δ* strain (Table 1). Second, treatment of the WT strain with rapamycin resulted in significant transcriptional induction in ceramidase promoter activity for both the *YDC1* and *YPC1* reporters, whereas such an induction was absent for both the *LAG1* and *LAC1* reporters (Figure 5B). The fact that derepression of the ceramidase enzymes is higher in *sch9Δ* cells than in WT cells treated with rapamycin might be due to the fact that our rapamycin treatment does not result in a complete inactivation of Sch9, especially in the BY4741 strain, which is more resistant to rapamycin treatment than most other backgrounds. Finally, the rapamycin-induced effect on the *YDC1* and *YPC1* reporters was abrogated in the *sch9Δ* strain (Figure 5C). As such, the effects on the Myc-tagged protein levels shown in Figure 4 are recapitulated on a transcriptional level by our lacZ results shown in Figure 5. Thus, Sch9 seems, indeed, to be the downstream effector of the TORC1 kinase in the transcriptional control of ceramidase expression. However, one may argue that the absence of rapamycin-induced expression of the *YDC1* and *YPC1* reporters in the *sch9Δ* strain may be due to an already complete derepression of promoter activity. Furthermore, induction of ceramidase promoter activity by rapamycin treatment in the WT strain might be due to Sch9-dependent and -independent effects, for instance through the Tap42 signaling branch of TORC1 (Smets et al., 2010). To further demonstrate that Sch9 is the principal mediator of the observed rapamycin effects, we used *SCH9* constructs in which specifically the five TORC1 phosphorylation sites were mutated (Urban et al., 2007). Mutation of these sites to alanine (*SCH9<sup>5A</sup>*) results in the expression of an inactive Sch9 protein that cannot be phosphorylated by

TORC1. On the other hand, mutation of these sites to aspartic (D) or glutamic (E) acid (*SCH9<sup>2D3E</sup>*) results in the expression of a variant of Sch9 that mimics a constitutively phosphorylated, and therefore active, Sch9, which cannot be inactivated by rapamycin treatment (Urban et al., 2007). We subcloned these *SCH9* variants, along with the wild-type *SCH9* gene, into the pRS415 vector to allow for coexpression with our *YDC1*- and *YPC1*-lacZ constructs in the *sch9Δ* strain. As shown in Figure 6, coexpression of the ceramidase lacZ constructs with wild-type *SCH9* in the *sch9Δ* strain can complement the high basal lacZ activity observed with the empty vector (pRS415), as well as restore rapamycin induction of promoter activity. Furthermore, expressing the inactive *SCH9<sup>5A</sup>* variant mimics the empty vector situation, demonstrating that phosphorylation of Sch9 by TORC1 is required for keeping basal promoter activities in check. Further induction by rapamycin is also abolished in cells expressing this *SCH9<sup>5A</sup>* construct. Expressing the phospho-mimic *SCH9<sup>2D3E</sup>* variant, on the other hand, results in basal promoter activities, comparable to those observed when expressing the wild-type *SCH9* gene (Figure 6). They are somewhat elevated compared with the wild-type gene, likely due to the slight differences in in vivo conformation between the phospho-mimic and truly phosphorylated Sch9. Still, comparing basal promoter activities of cells expressing *SCH9<sup>5A</sup>* and *SCH9<sup>2D3E</sup>* clearly demonstrates the importance of phosphorylation of the TORC1-dependent residues of Sch9 in regulating ceramidase promoter activity. Intriguingly, rapamycin-mediated induction of *YDC1*- and *YPC1*-lacZ activity is completely lost in cells expressing the *SCH9<sup>2D3E</sup>* variant, indicating that this induction by rapamycin requires a loss in phosphorylation of Sch9 by TORC1. Also, these results argue against additional effectors besides Sch9 in mediating the rapamycin effect.

In conclusion, due to the tight correlation between the effects observed in the lacZ experiments and the determination of protein levels (summarized in Table 1), our results point to the existence of a nutrient-dependent transcriptional response in which the TORC1–Sch9 signaling pathway acts to repress the expression of the ceramidase enzymes (*YDC1* and *YPC1*). In addition, TORC1-independent regulation mechanisms exist that affect the transcriptional regulation of the genes encoding the ceramide synthases (*LAG1* and *LAC1*), thereby constituting an independent homeostatic mechanism controlling sphingolipid balance. Whether the latter mechanism is also independent of Sch9 remains to be established. Indeed, despite being a major downstream effector of TORC1, Sch9 also performs functions independent of this upstream regulator (Pascual-Ahuir and Profitt, 2007; Smets et al., 2008).

### Sch9 has a regulatory role in the metabolism of complex sphingolipids

Because Sch9 proved to have a significant effect on the LCB(P)/ceramide balance, we set out to test how the complex sphingolipid profile was affected by deletion of *SCH9*. To this end, we measured the levels of the three major inositol phosphosphingolipid classes, namely IPC, mannosylinositolphosphoryl ceramide (MIPC), and mannosyldiinositolphosphoryl ceramide (M(IP)<sub>2</sub>C), in membranes of WT and *sch9Δ* cells. This revealed that the *sch9Δ* mutant combined relative reduced levels of IPC with increased levels of MIPC and M(IP)<sub>2</sub>C (Figure 7). Intriguingly, a recent lipidomic approach indicated that as yeast cells go into the stationary phase, IPC levels drop, whereas MIPC levels increase and M(IP)<sub>2</sub>C levels remain constant (Klose et al., 2012). The net result is the same as we observe upon deletion of *SCH9*, that is, a relative decrease in IPC levels combined with a relative increase in MIPC and M(IP)<sub>2</sub>C levels. Thus, the complex sphingolipid profile of a *sch9Δ* strain reflects that of a WT

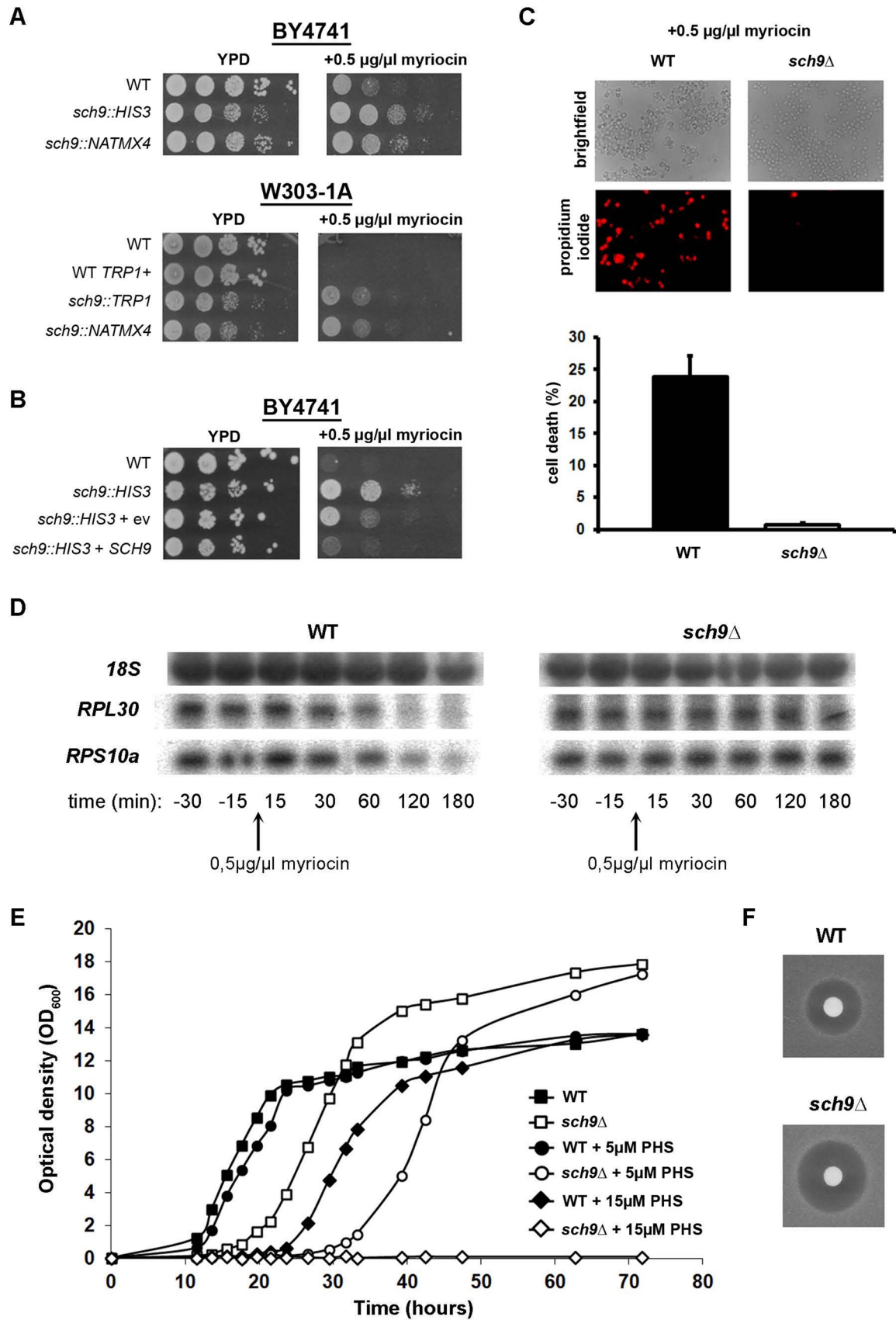


**FIGURE 2:** Deletion of *SCH9* confers resistance to myriocin and increases sensitivity to phytosphingosine and aureobasidin A. (A) Serial dilutions of exponentially growing wild-type and *sch9Δ* cells of two different genetic backgrounds (BY4741 and W303-1A) and with different markers were spotted on YPD and on YPD containing 0.5 µg/ml myriocin. (B) Serial dilutions of *sch9Δ* cells (BY4741 background, JW 01 306), transformed with YEpLac195 (ev) or

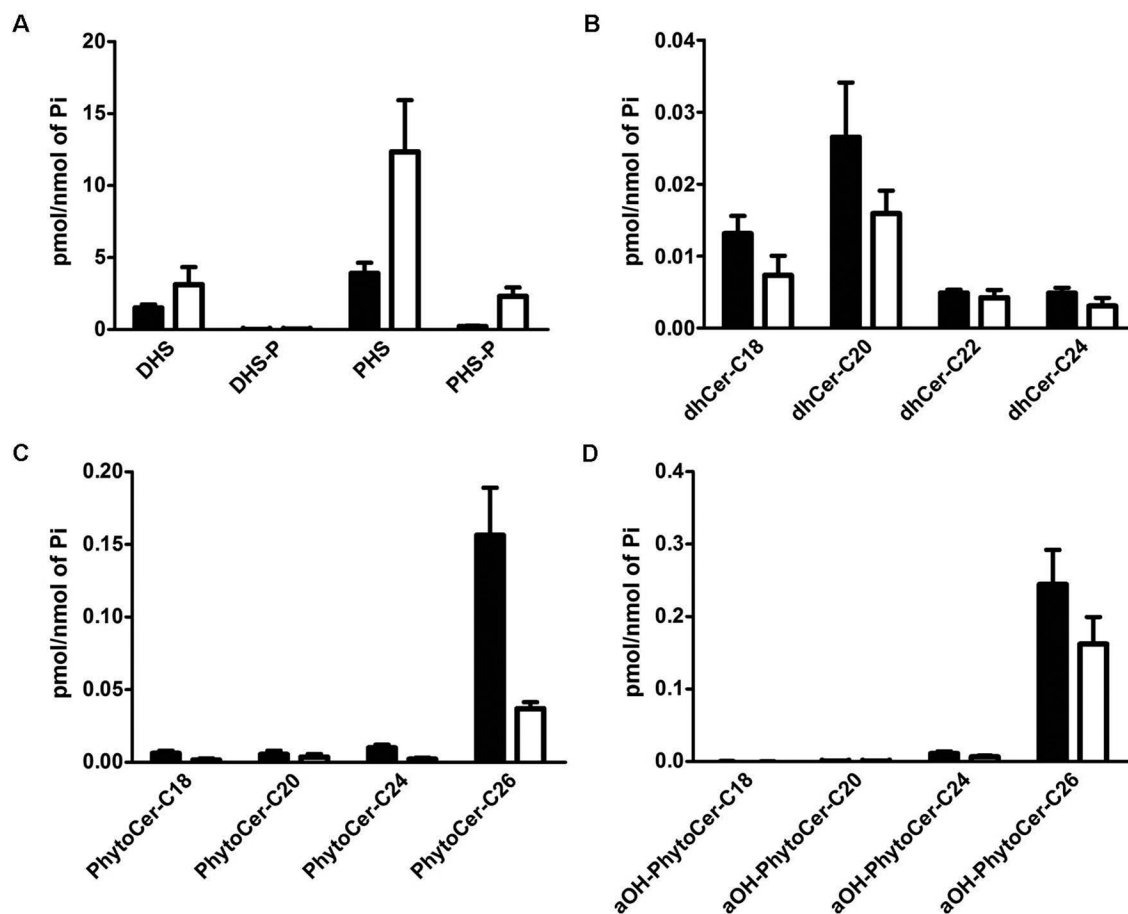


**FIGURE 3:** The levels of LCBs, LCB-phosphates, and ceramides are altered in *sch9Δ* cells. Sphingolipids were purified from wild-type (W303-1A; closed bars) and *sch9Δ* (JW 01 418; open bars) cells growing exponentially in YPD medium, analyzed by LC-MS, and normalized by organic phosphates: (A) Phytosphingosine and dihydrosphingosine bases and their phosphates, (B) dihydroceramide species (DHcer) with acyl chains of different length, (C) phytoceramide species (PhytoCer) with acyl chains of different length, and (D)  $\alpha$ OH-PhytoCer with acyl chains of different length. The results are mean values  $\pm$  SD of lipid measurements from three independent cultures measured in duplicate.

yeast strain in stationary phase, consistent with the model that Sch9 activity signals the presence of nutrients (Urban *et al.*, 2007). The reduction of IPC could be explained by the reduced content of (phyto)ceramides, which serve as precursors. However, the increment in the levels of mannosylated sphingolipids suggests an additional regulatory role for Sch9 in the biosynthesis or turnover of mannosylated sphingolipids.

### Sch9 affects the mitochondrial translocation of Isc1

To further decipher the connection between Sch9 and complex sphingolipid synthesis, we performed a genetic analysis on myriocin resistance of an *sch9Δ* strain lacking additional genes involved in the synthesis of complex sphingolipids. Results indicated that

complex sphingolipids may also contribute to myriocin resistance (Supplemental Figure S1A). Specifically interesting to us was the observation that additional deletion of *ISC1* resulted in an increase in myriocin resistance of the *sch9Δ* strain (Figure 15B). This result indicates a functional link between Sch9 and Isc1, the inositol phosphosphingolipid phospholipase C, which hydrolyses IPC, MIPC, and M(IP)<sub>2</sub>C back into (phyto)ceramides (Sawai *et al.*, 2000). We first examined whether Sch9 might influence Isc1 protein levels, similar to the situation seen for the enzymes involved in de novo ceramide synthesis. To this end, we constructed WT and *sch9Δ* strains expressing a chromosomally encoded, Myc-tagged version of Isc1. Determination of the levels of Isc1-Myc in exponentially growing cells demonstrated that deletion of *SCH9* or treatment of

YEplac195/*SCH9* (*SCH9*) were spotted on YPD and on YPD containing 0.5  $\mu$ g/ml myriocin. (C) Exponentially growing wild-type (W303-1A background) and *sch9Δ* (JW 01 418) cells were treated for 2 h with 0.5  $\mu$ g/ml myriocin and stained with propidium iodide to visualize dead cells. Results are mean values  $\pm$  SD of three independent cultures. At least 200 cells were counted for each experiment. (D) Northern blot analysis of the myriocin (0.5  $\mu$ g/ml)-induced transcriptional response in wild-type (W303-1A) and *sch9Δ* (JW 00 035) cells of two typical ribosomal protein genes, *RPS10a* and *RPL30*. *18S* was used as a loading control. Samples were taken at the indicated time points. (E) Growth of wild-type (W303-1A; closed symbols) and *sch9Δ* (JW 00 035; open symbols) cells was monitored during growth on YPD without or with supplementation of the indicated amounts of PHS. To dissolve PHS, 0.0015% of the detergent Nonidet P-40 was added together with PHS. (F) Sensitivity of wild-type (W303-1A) and *sch9Δ* (JW 00 035) cells to aureobasidin A (1 mg/ml), as assessed via a growth-inhibitory halo assay on YPD agar plates.

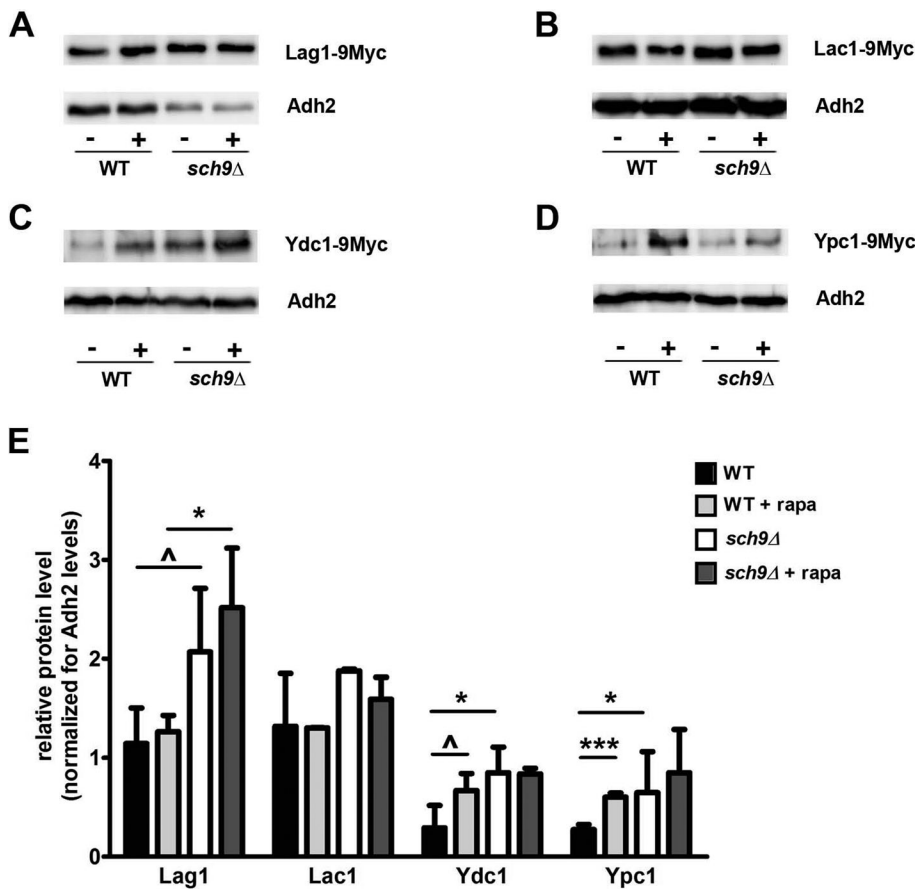


**FIGURE 4:** Sch9 affects protein levels of enzymes involved in de novo ceramide synthesis and breakdown. Genes encoding the enzymes of ceramide synthase (*LAG1* and *LAC1*) or ceramidase (*YDC1* or *YPC1*) were genomically tagged with a 9Myc tag in both WT BY4741 and *sch9Δ* (JW 03 038) strains. Overnight precultures were inoculated at initial OD<sub>600</sub> of 0.3 and grown to OD<sub>600</sub> of 2.0, after which a sample was withdrawn for protein extraction (noted as –). The remainder of the culture was treated with 200 nM rapamycin and grown for an additional 1 h, after which a second sample for protein extraction was taken (noted as +). After TCA protein extraction, equal protein amounts were run on a SDS–PAGE. Tagged enzymes were detected using an anti-Myc antibody; the yeast *Adh2* serves as an internal control. Representative results for Western blots are shown for (A) Lag1-9Myc, (B) Lac1-9Myc, (C) Ydc1-9Myc, and (D) Ypc1-9Myc. Signals for Myc detection were quantified and normalized for *Adh2* levels. Average results of two or three independent cultures are shown in E, with SD shown as error bars. Statistical significance was determined by unpaired t tests for effects between the WT and *sch9Δ* strains, and paired t tests for effects of rapamycin. Because several experimental manipulations in Western blot experiments, such as variations in blotting efficiency, antibody activity, and so on, increase variability not related to the intrinsic properties of the protein samples, we set the threshold for statistical significance at  $p < 0.1$  instead of the usual threshold of  $p < 0.05$ . Results of the t tests are shown as  $^{\wedge}p < 0.1$ ,  $*p < 0.05$ , and  $***p < 0.001$ .

cells with rapamycin did not alter Isc1-Myc levels (Supplemental Figure S2).

Previous studies demonstrated that Isc1 gains activity during the diauxic shift, when it translocates from the ER to the outer membrane of mitochondria, where the enzyme is required to produce a subset of phytoceramides, especially  $\alpha$ OH-PhytoCer-C<sub>26</sub> (Vaena de Avalos *et al.*, 2004, 2005; Kitagaki *et al.*, 2007). Because Sch9 plays a pivotal role in the diauxic shift transition (Pedruzzi *et al.*, 2003; Roosen *et al.*, 2005), we set out to monitor and compare the intracellular localization of Isc1 in WT and *sch9Δ* cells during different growth phases. Initially, we used a galactose-induced Isc1–green fluorescent protein (GFP) expression construct in combination with a red fluorescent mitochondrial marker protein.

of Isc1 in postdiauxic-phase cells in both glucose- and galactose-grown cells.

### Implications of the functional interaction between Sch9 and Isc1 for yeast longevity

Consistent with Sch9 acting as a regulator of Isc1, several studies documented that Isc1 plays a role in well-known Sch9-dependent phenotypes, including diauxic shift reprogramming and respiration, oxidative stress resistance, and the determination of longevity (Almeida *et al.*, 2008; Kitagaki *et al.*, 2009; Barbosa *et al.*, 2011). Intriguingly, although loss of Sch9 is known to trigger increased resistance to oxidants and increased chronological life span (Fabrizio *et al.*, 2001; Wei *et al.*, 2009), loss of Isc1 is associated with a higher

In agreement with previous work, we observed Isc1-GFP localization at the ER in WT and *sch9Δ* cells during exponential growth (Vaena de Avalos *et al.*, 2004), with almost no sign of mitochondrial colocalization (Supplemental Figure S3). In the post-diauxic growth phase, Isc1-GFP mainly colocalized with mitochondria in WT cells, whereas in *sch9Δ* cells, Isc1-GFP remained mostly localized at the ER (Supplemental Figure S3), indicating involvement of Sch9 in mitochondrial translocation of Isc1 on galactose-containing medium. We were curious as to whether Isc1 also translocates to the mitochondria in the postdiauxic phase of cells grown on glucose-containing medium and whether deletion of *SCH9* would have a similar effect under these conditions. Furthermore, because we determined our sphingolipid profiles for cells growing on glucose as the carbon source, studying the intracellular localization of Isc1 in cells grown on glucose could be directly related to our observed sphingolipid profiles. To this end, we subcloned the *ISC1*-GFP construct behind its own promoter. In addition, we made two parallel analyses of Isc1-GFP localization: in a first series of experiments, we scored colocalization of Isc1 with an ER-specific mCherry marker (Figure 8A), whereas colocalization with mitochondria was analyzed in a second series of experiments using a mCherry marker targeted to the mitochondria (Figure 8B). For both the WT and *sch9Δ* strains, we saw that in cells growing exponentially on glucose, Isc1 localized almost exclusively in the perinuclear and cortical ER (Figure 8A), without any significant colocalization with mitochondria (Figure 8B). When scoring colocalization of Isc1 with the ER in cells in the postdiauxic phase, we noticed a higher retention of Isc1 in the ER in *sch9Δ* cells than in WT cells (Figure 8A). Consistent with this observation, postdiauxic-phase WT cells showed more colocalization of Isc1 with the mitochondrial marker than *sch9Δ* cells (Figure 8B). Therefore we conclude that deletion of *SCH9* impairs mitochondrial translocation

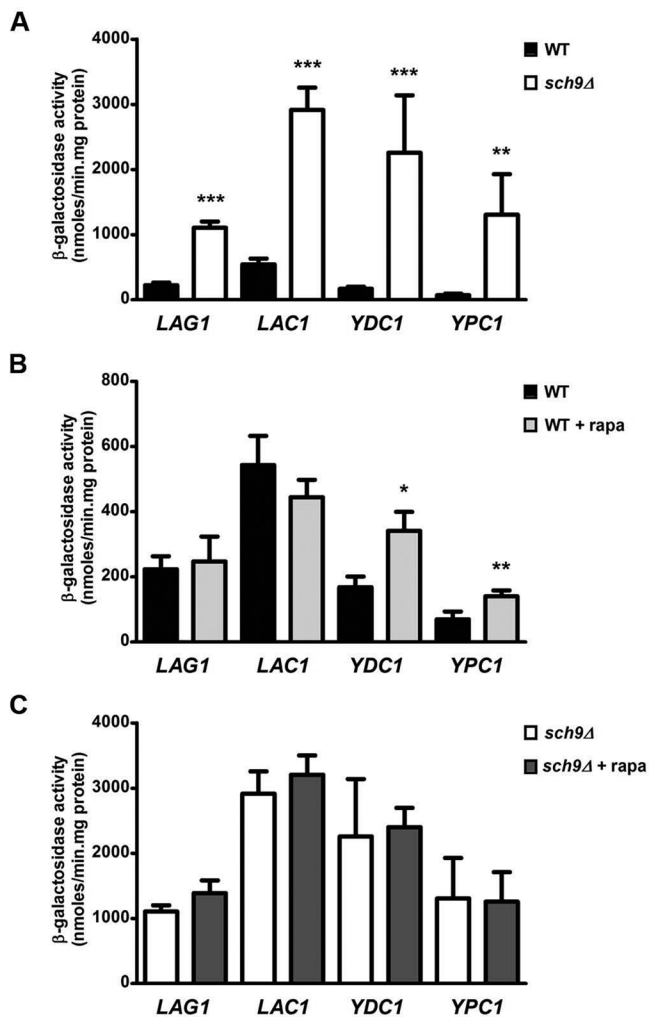


**FIGURE 5:** Transcriptional control by Sch9 of genes encoding enzymes involved in de novo ceramide synthesis and breakdown. Promoters of genes *LAG1*, *LAC1*, *YDC1*, and *YPC1* were cloned into the lacZ reporter plasmid YEp357 as described in *Materials and Methods* and transformed into the WT BY4741 and *sch9Δ* (JW 03 038) strains. Precultures were grown overnight in SD-URA, inoculated into YPD medium, and grown for 6–7 h, after which part of the culture was treated with 200 nM rapamycin. After 1 h, samples of treated and untreated cells were pelleted at 4°C and stored at –80°C. Protein extracts were prepared, and specific activities were determined. Results are expressed as mean of four independent transformants, with SD noted as error bars. Results displayed in A indicate a significant increase in lacZ activities in the *sch9Δ* strain compared with the WT strain (\*\* $p < 0.01$ , \*\*\* $p < 0.001$ , unpaired t test). Rapamycin-dependent effects in WT and *sch9Δ* cells are separately displayed in B and C, respectively, for extra clarity. Only in the WT strain there was a significant increase in *YDC1*- and *YPC1*-lacZ activities observed after addition of rapamycin to the cells (\* $p < 0.05$ , \*\* $p < 0.01$ , paired t test).

oxidative stress sensitivity and reduced chronological life span (Almeida *et al.*, 2008). To further elaborate on the functional interaction between Sch9 and Isc1, we determined the chronological life span of mutants lacking *SCH9* and/or *ISC1* (Figure 9A). In agreement with previous published results, we observed an increase in life span in the *sch9Δ* mutant as compared with the WT strain (Fabrizio *et al.*, 2001; Wei *et al.*, 2009), whereas the *isc1Δ* mutant displayed reduced viability (Kitagaki *et al.*, 2009; Barbosa *et al.*, 2011). In parallel with viability, we assessed the levels of cellular reactive oxygen

species (ROS) under the same conditions, as an increase in oxidative stress plays a major role in determining viability in stationary phase. As compared with WT cells, the level of ROS was already elevated in exponential *isc1Δ* cells, and this difference became more pronounced when the cells enter the stationary phase (Figure 9, B and C). In *sch9Δ* cells, the level of ROS also increased during growth, but here the amount of ROS was always significantly lower than in WT cells. Of interest, the additional deletion of *SCH9* in the *isc1Δ* mutant restored the ROS production to levels comparable to those of WT cells (Figure 9, B and C). In line with these reductions in ROS levels, survival of the *sch9Δ isc1Δ* double mutant increased compared with the *isc1Δ* strain (Figure 9A). Finally, the decreased chronological life span of cells lacking Isc1 was shown to be due to increased apoptotic cell death (Almeida *et al.*, 2008). We confirmed the involvement of apoptosis in mediating the accelerated cell death of *isc1Δ* cells by staining yeast cells with the cell death markers of apoptosis and necrosis (annexin/PI costaining; Supplemental Figure S4). We also showed that deletion of *SCH9* decreases apoptotic cell death, independent of the presence or absence of *ISC1*, correlating with the decreased oxidative stress observed in these strains. Linking these viability data with our observation that Sch9 is required for proper mitochondrial translocation of Isc1 in postdiauxic-phase cells is a delicate matter. Because Isc1-mediated sphingolipid metabolism in mitochondria is required for proper mitochondrial function and viability in stationary phase (Almeida *et al.*, 2008; Kitagaki *et al.*, 2009), this would indicate a prosurvival function of Sch9 in stimulating Isc1 activity, which contradicts the increased life span of cells deleted for *SCH9* (Figure 9A). On the other hand, decreased mitochondrial translocation of Isc1 in the *sch9Δ* mutant implies a reduction of mitochondrial ceramide species produced by Isc1 in the postdiauxic phase of *sch9Δ* cells (Vaena de Avalos *et al.*, 2005; Kitagaki *et al.*, 2007). Several studies showed that ceramides can interact directly with mitochondria, thereby increasing mitochondrial membrane permeability (Birbes *et al.*, 2001; Siskind *et al.*, 2002, 2005; Chipuk *et al.*, 2012; Rego *et al.*, 2012) and disrupting electron transport, resulting in elevated ROS levels (Garcia-Ruiz *et al.*, 1997; Guduz *et al.*, 1997; Di Paola *et al.*, 2000). As such, impaired Isc1 translocation might be responsible for part of the increased longevity observed in a *sch9Δ* strain, although this antisurvival function of Isc1 does not fit with the loss of viability upon deleting *ISC1* in the WT or *sch9Δ* strain (Figure 9A). Clearly, more work is needed to further characterize the molecular connections between Sch9 and Isc1 functions. For instance, although it was proven that Isc1 activity increases upon translocation to the mitochondria (Vaena de Avalos *et al.*, 2004, 2005), it may also possess (basal) enzymatic activity at the ER. Future studies may test the effect of Sch9 specifically on the enzymatic activity of Isc1 at these different cellular locations. Furthermore, due to the plethora of ceramide species, it is conceivable that specific ceramide species, possibly generated at different intracellular locations, mediate different cellular responses, thereby regulating either survival or death, depending on the cellular context (Hannun and Obeid, 2011; Matmati *et al.*, 2013). Of interest, the complex sphingolipids, whose profile is also altered by deletion of *SCH9*, were recently demonstrated to influence yeast viability, independent of their ceramide precursors (Kajiwara *et al.*, 2012). As such, these species should not be overlooked when building a model for the cell death/survival mechanisms operating in yeast cells.

## DISCUSSION

### Sch9 is a regulator of sphingolipid metabolism

Regulation of the sphingolipid rheostat is essential for yeast cells to ensure proper growth and survival properties (Dickson, 2010).



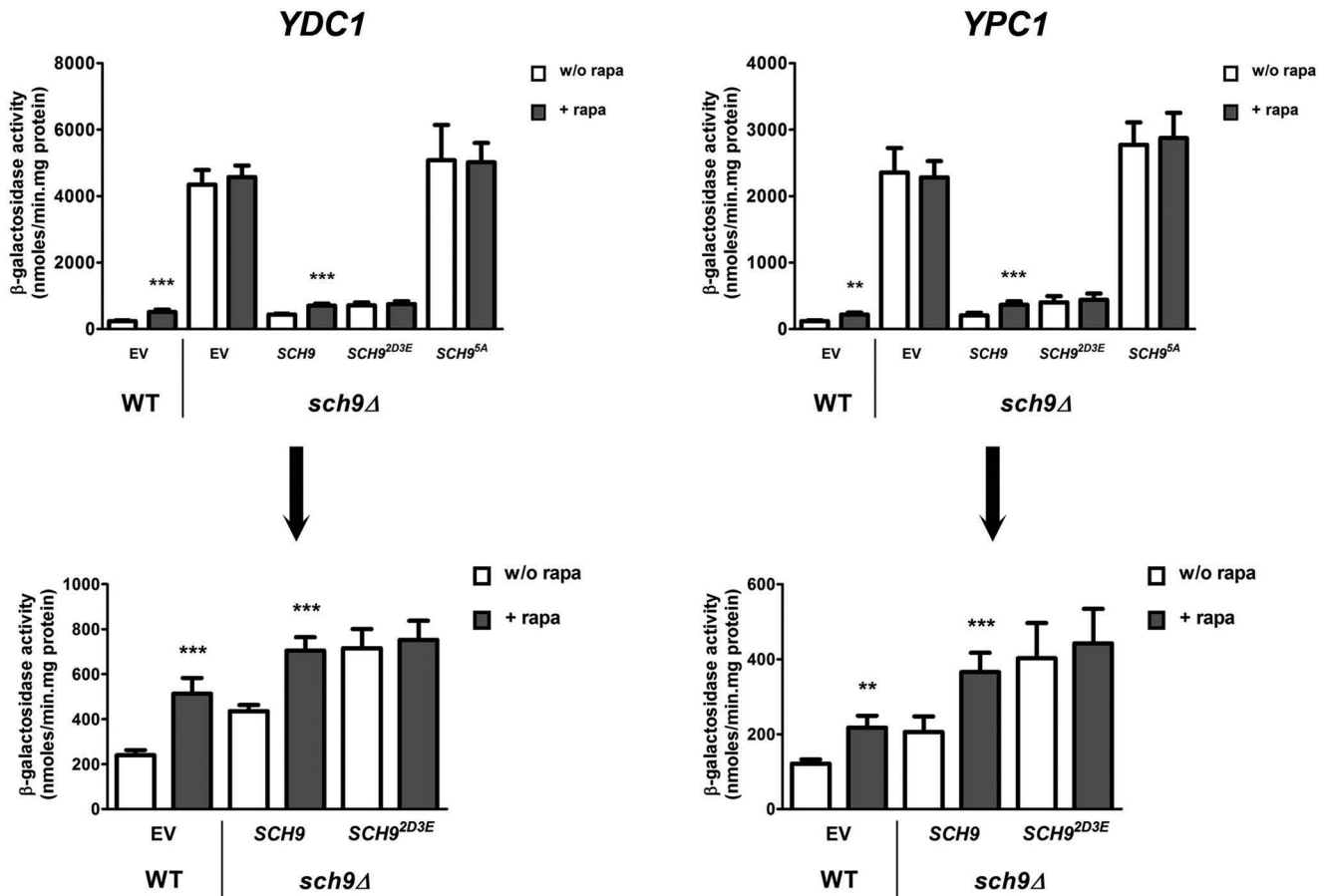


**FIGURE 6:** The rapamycin-induced effects on *YDC1* and *YPC1* lacZ activity are mediated by Sch9. LacZ activities of the *YDC1* (left) and *YPC1* (right) promoters was assessed in the *sch9Δ* strain (JW 03 038) coexpressing the empty vector (EV, pRS415), the wild-type *SCH9* gene, or one of the *SCH9* mutant genes in which its TORC1 phosphorylation sites are mutated to either alanine (*SCH9<sup>5A</sup>*) or glutamic/aspartic acid residues (*SCH9<sup>2D3E</sup>*). The WT strain (BY4741) coexpressing the EV was taken as an additional control. Precultures were grown overnight in SD-URA-LEU, inoculated into YPD medium, and grown for 6–7 h, after which part of the culture was treated with 200 nM rapamycin. After 1 h, samples of treated and untreated cells were pelleted at 4°C and stored at –80°C. Protein extracts were prepared, and specific activities were determined. Results are expressed as mean of four independent transformants, with SD noted as error bars. Top: all results in one graph. Bottom: for clarity, selective omission of results of conditions that mimic the condition of the *sch9Δ* strain with the EV. Results for both promoters are equivalent, in that the *SCH9<sup>5A</sup>* construct mimics the absence of *SCH9* in its high basal lacZ activity and no induction by rapamycin. The *SCH9<sup>2D3E</sup>* construct, on the other hand, gives basal lacZ activities compared with the *SCH9* control strain, although induction by rapamycin is lost due to the inability of the *Sch9<sup>2D3E</sup>* protein to be inhibited by loss of TORC1 activity. Statistical significance of rapamycin addition for each construct was assessed by a paired t test (\*\**p* < 0.01, \*\*\**p* < 0.001).

Therefore it is not surprising that this sphingolipid balance changes when nutrient conditions alter. In this study, we observed that, during growth, the *sch9Δ* strain displays sphingolipid profiles described for cells in stationary phase. Indeed, compared with the WT strain, *sch9Δ* cells accumulate LCB(P)s and have decreased (phyto)ceramide levels and an altered profile of complex sphingolipids, which is similar to cells entering into stationary phase (Klose *et al.*, 2012; Lester *et al.*, 2013). The specific increase of mannosylated sphingolipid species compared with IPC levels indicates that Sch9 has additional inputs into complex sphingolipid synthesis, apart from its role in maintaining the LCB(P)/ceramide balance. Interestingly, TORC1 inhibition has been reported to stimulate complex sphingolipid synthesis through Npr1-dependent phosphorylation of the Orm1/2 proteins (Shimobayashi *et al.*, 2013). The molecular mechanism behind this phenotype is unknown, although it was shown to be independent of SPT activity. Given that these results were

obtained by short-term rapamycin treatment, steady-state levels of complex sphingolipids may thus be regulated by TORC1 through both the Sit4-Npr1 effector branch and the Sch9 effector branch, the latter being supported by this work.

Concerning the LCB(P)/ceramide rheostat, we demonstrate a novel mechanism in which Sch9 controls the presence of the Ydc1 and Ypc1 ceramidase enzymes. Using promoter-lacZ reporter constructs, we demonstrate that Sch9 performs this function by acting at the transcriptional level, with deletion of *SCH9* resulting in a significant derepression of *YDC1* and *YPC1* expression. Treating WT cells with rapamycin, which inhibits the nutrient-dependent kinase TORC1, also results in derepression of *YDC1* and *YPC1*, and we show that this effect is mediated by Sch9, which is known to act as a downstream effector of TORC1 (Urban *et al.*, 2007). Therefore we conclude that signaling through the TORC1–Sch9 pathway during nutrient-rich conditions serves to repress transcription of the *YDC1*

Protein <sup>a</sup>	Fold increase	Significance	lacZ construct <sup>b</sup>	Fold increase	Significance
<b>Fold increase in <i>sch9Δ</i> vs. WT strain</b>					
Lag1-9Myc	1.8	^	LAG1pr	4.9	***
Lac1-9Myc	1.4	ns	LAC1pr	5.4	***
Ydc1-9Myc	2.9	*	YDC1pr	13.4	***
Ypc1-9Myc	2.4	*	YPC1pr	18.7	**
<b>Fold increase after addition of rapamycin to WT cells</b>					
Lag1-9Myc	1.1	ns	LAG1pr	1.1	ns
Lac1-9Myc	1.0	ns	LAC1pr	0.8	ns
Ydc1-9Myc	2.3	^	YDC1pr	2.0	*
Ypc1-9Myc	2.2	***	YPC1pr	2.0	**
<b>Fold increase after addition of rapamycin to <i>sch9Δ</i> cells</b>					
Lag1-9Myc	1.2	ns	LAG1pr	1.3	ns
Lac1-9Myc	0.8	ns	LAC1pr	1.1	ns
Ydc1-9Myc	1.0	ns	YDC1pr	1.1	ns
Ypc1-9Myc	1.1	ns	YPC1pr	1.0	ns

Statistical significance was determined using an unpaired t test for the effects of *sch9Δ* vs. WT strain, and paired t tests for the effects of rapamycin addition. Statistical significance: ^ $p < 0.1$  (only used for protein levels), \* $p < 0.05$ , \*\* $p < 0.01$ , and \*\*\* $p < 0.001$ .

<sup>a</sup>Analysis of results shown in Figure 4.

<sup>b</sup>Analysis of results shown in Figure 5.

**TABLE 1:** Effects of *SCH9* deletion and rapamycin addition on protein levels and lacZ promoter constructs.

and *YPC1* ceramidase-encoding genes. We also observed TORC1-independent effects on the expression of the ceramide synthase genes *LAG1* and *LAC1* in the *sch9Δ* strain. However, we cannot discriminate between whether this represents a true Sch9-dependent, TORC1-independent, signaling event or is due to additional, Sch9-independent homeostatic mechanisms that counteract the significant increased ceramidase presence in the *sch9Δ* strain. Identification of the transcription factors involved in these processes, which is currently being pursued, will help to shed light on this issue.

It is intriguing that, besides TORC1, multiple in vitro and in vivo studies show that Sch9 activity is also regulated independently by the LCB (PHS)-dependent Pkh1/2 kinases (Roelants *et al.*, 2004; Liu *et al.*, 2005; Urban *et al.*, 2007; Voordeckers *et al.*, 2011; Huang *et al.*, 2012). According to this model, if PHS drops (e.g., by myriocin treatment), Sch9 activity will also drop due to reduced phosphorylation by Pkh1/2. This would lead to increased ceramidase action, helping to restore internal LCB pools. Therefore Sch9 comprises a major gatekeeper of sphingolipid homeostasis, optimizing ceramidase activity by integrating information on internal LCB (PHS) levels through Pkh1/2, as well as information on nutritional status via TORC1, thereby adjusting sphingolipid metabolite levels to cellular needs. Given that Orm1/2-mediated regulation of sphingolipid metabolism was shown to be mainly regulated via (rapid) Orm1/2 phosphorylation, the Sch9-mediated transcriptional response may comprise a complementary mechanism, operating somewhat more slowly, as it is dependent on transcription, although probably essential to generate major long-term changes in the sphingolipid rheostat.

#### Altered sphingolipid levels and longevity in *sch9Δ* cells

A well-established phenotype of the *sch9Δ* strain is its increased survival during stationary phase (Fabrizio *et al.*, 2001; Wei *et al.*, 2009), and much research has been performed to elucidate the mechanisms behind this phenotype. Sphingolipids are also crucial regulators of cell viability, and it has been shown that in higher

eukaryotes, the balance in intermediary sphingolipid signaling metabolites, the so-called sphingolipid rheostat, has an important function in cell survival, disease and senescence (Olivera *et al.*, 1999; Levade *et al.*, 2002; Hait *et al.*, 2006; Saddoughi *et al.*, 2008; Breslow and Weissman, 2010; Dickson, 2010; Bikman and Summers, 2011; Van Brocklyn and Williams, 2012). Therefore it is not surprising that the altered sphingolipid profile we describe for *sch9Δ* cells may have important contributions to the increased life span of this strain.

The increased survival of the *sch9Δ* strain is reported to be partly due to increased mitochondrial function and respiration during growth (Lavoie and Whiteway, 2008; Pan and Shadel, 2009; Pan *et al.*, 2011). Of interest, the elevated PHS-P levels of *sch9Δ* cells we demonstrated in this study might be crucial for this process, as cellular PHS-P have been implicated in the control of the HAP complex transcription factor (Coward *et al.*, 2010), which regulates mitochondrial respiration. As such, our results would provide the missing mechanistic link between Sch9 and the Hap4 transcription factor, which was shown to be essential for the increased cellular respiration in *sch9Δ* cells (Lavoie and Whiteway, 2008).

The decreased ceramide levels may also contribute to the increased life span of the *sch9Δ* strain. Indeed, evidence indicates that ceramides can induce a mitochondrial cell death pathway in yeast, which seems to involve increasing mitochondrial membrane permeability (Carmona-Gutierrez *et al.*, 2011; Rego *et al.*, 2012). In addition, ceramides exert proapoptotic effects via ceramide-activated protein phosphatases, such as Sit4 in yeast (Nickels and Broach, 1996; McCourt *et al.*, 2009; Barbosa *et al.*, 2011). In addition to the aforementioned effect of Sch9 on the de novo synthesis of ceramides, we demonstrate that Sch9 is required for the proper mitochondrial localization of *Isc1* in postdiauxic cells, which, to our knowledge, is the first report of a protein required for *Isc1* translocation (Vaena de Avalos *et al.*, 2004, 2005; Kitagaki *et al.*, 2007). Given that this translocation of *Isc1* is blocked in *sch9Δ* cells, this may abrogate the production of a specific mitochondrial ceramide pool,

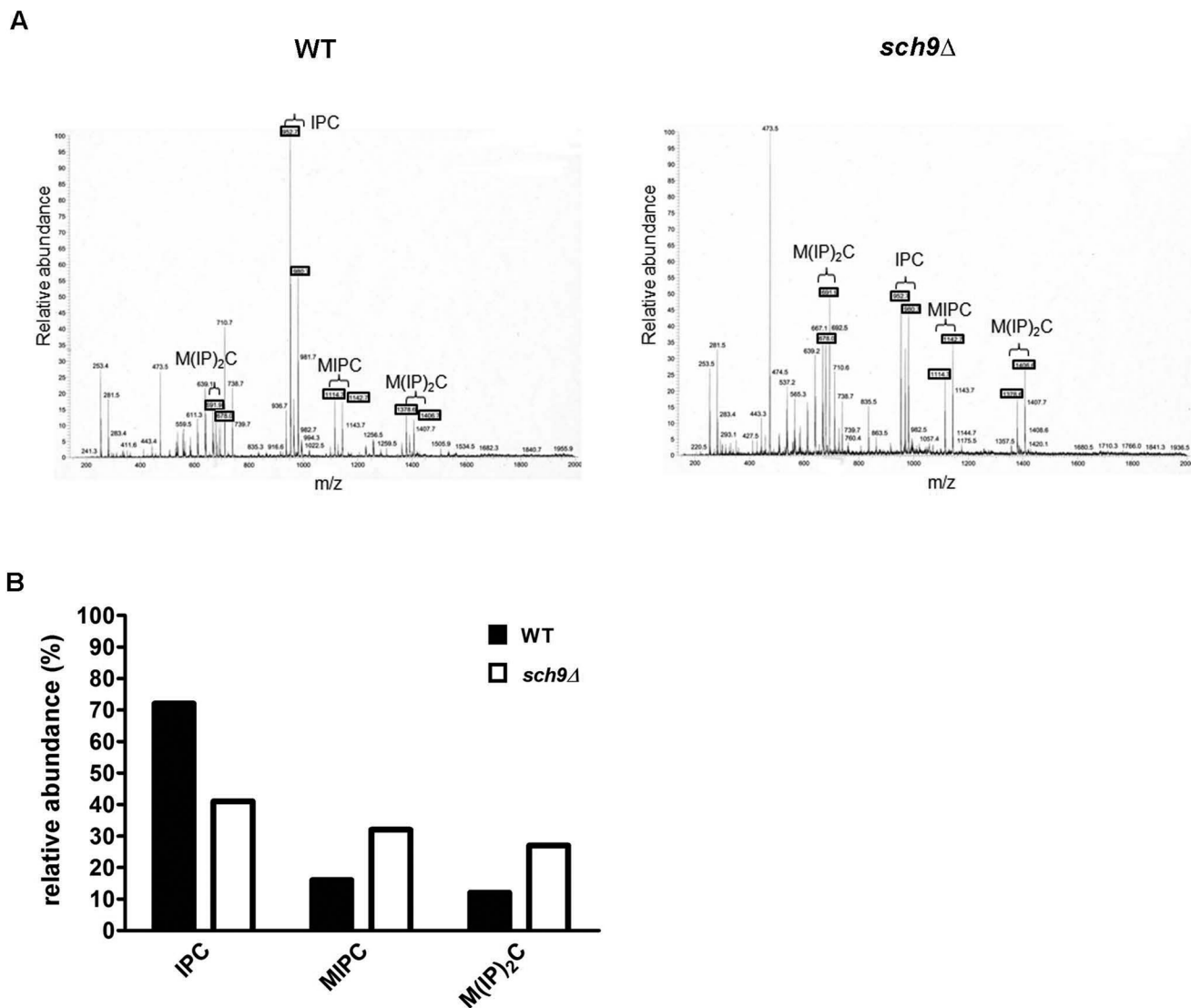


**FIGURE 7:** The complex sphingolipid profile is changed in *sch9Δ* cells. Negative-ion ESI/MS spectra of complex sphingolipids from wild-type (W303-1A; open bars) and *sch9Δ* (JW 01 418; closed bars) mutants. Sphingolipids were purified from wild-type and *sch9Δ* cells growing exponentially in YPD medium. The three different classes of complex sphingolipids—IPCs, MIPCs, and M(IP)<sub>2</sub>Cs—are indicated. (A) Representative spectrum from two independent measurements. (B) Quantifications of relative levels.

which could contribute to apoptotic cell death, as demonstrated in both yeast and mammals (Birbes *et al.*, 2001; Chipuk *et al.*, 2012; Rego *et al.*, 2012). Still, we and others have shown that loss of *ISC1* impairs survival during stationary phase (Almeida *et al.*, 2008; Kitagaki *et al.*, 2009; Barbosa *et al.*, 2011), indicating that *Isc1*-mediated ceramide production can elicit prosurvival and antisurvival programs, depending on specific cellular conditions. Finally, since *Sch9* activity is proposed to decline upon nutrient depletion, this indicates that *Sch9* affects the translocation of *Isc1* indirectly. Given that *sch9Δ* cells were shown to have altered mitochondrial properties, such as reduced superoxide production, in stationary phase (Pan and Shadel, 2009; Pan *et al.*, 2011), our experimental observations support a model in which mitochondrial ROS production may provide the cellular signal for *Isc1* translocation.

In conclusion, we show that the TORC1–*Sch9* signaling branch controls sphingolipid homeostasis by controlling the expression of the ceramidase enzymes. Given that transcriptional regulation mechanisms of sphingolipid metabolism are still largely elusive (Breslow and Weissman, 2010), it will be of interest to see whether

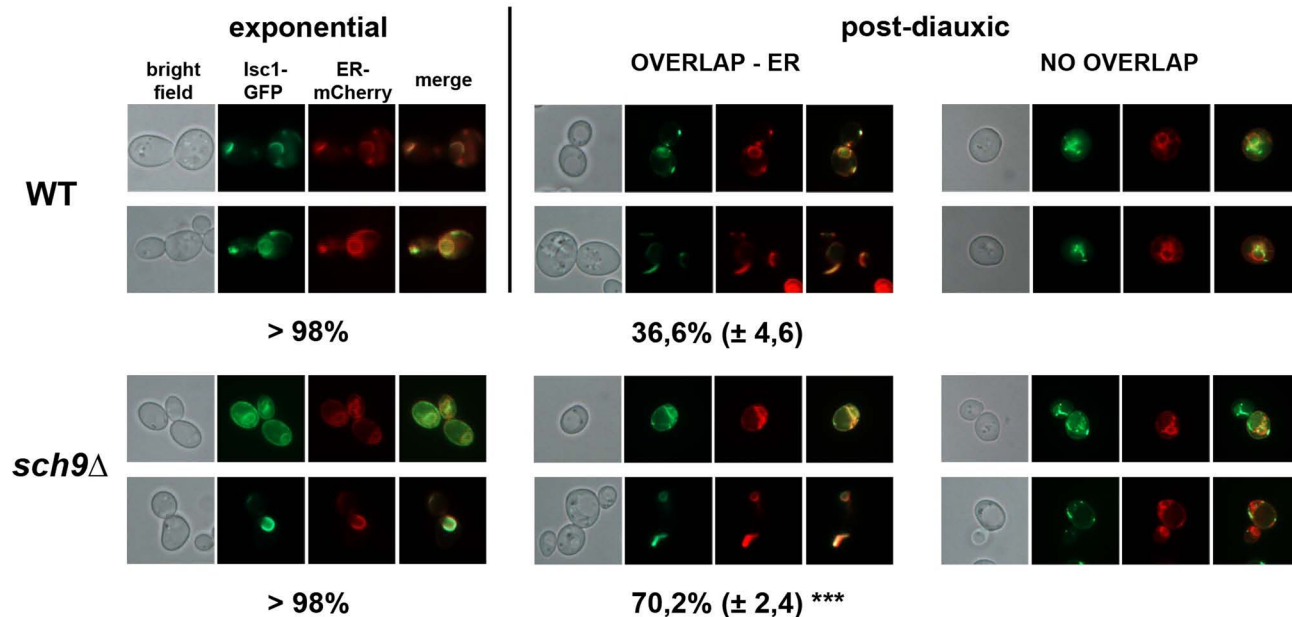
the mechanisms described here are conserved in higher eukaryotes. Furthermore, the altered sphingolipid profile exhibited by the *sch9Δ* strain provides additional molecular links that help explain the extended life span of this strain. As such, it appears that changing the sphingolipid balance in yeast by tipping it in favor of the (LCBs and) LCBPs, concomitant with decreased ceramide levels, results in lower apoptosis and increased survival, which in many ways is similar to what is seen for mammalian cells (Olivera *et al.*, 1999; Levade *et al.*, 2002; Hait *et al.*, 2006; Saddoughi *et al.*, 2008; Bikman and Summers, 2011; Van Brocklyn and Williams, 2012). Given this conserved nature of the role of sphingolipid signaling in eukaryotic cells, yeast may continue to serve as an important model system for higher eukaryotes.

## MATERIALS AND METHODS

### Materials, yeast strains, plasmids, and growth media

*S. cerevisiae* strains and plasmids used in this study are listed in Supplemental Tables S1 and S2, respectively. Deletion strains were made using PCR-derived deletion cassettes (Brachmann *et al.*,

## A Overlap Isc1-GFP with ER (Kar2-mCherry-HDEL)



## B Overlap Isc1-GFP with mitochondria (mt-mCherry)

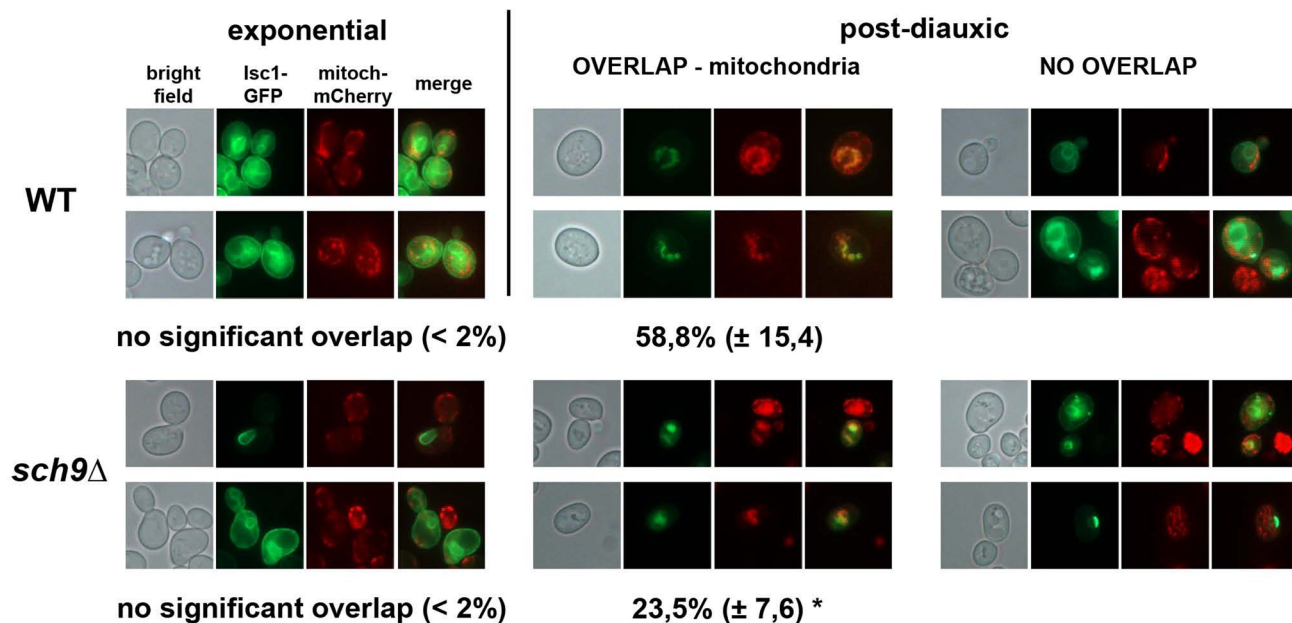


**FIGURE 8:** Fluorescence microscopic analysis of the intracellular localization of Isc1. Intracellular localization of Isc1-GFP expressed from its own promoter (plasmid FBp708) in wild-type (BY4741) and *sch9Δ* (JW 03 038) cells was examined by assessing colocalization with a mCherry marker targeted to the ER or the mitochondria. Cells precultured on SD-URA-LEU were inoculated in fresh YPD medium (2% glucose) at an initial OD<sub>600</sub> of 0.5. Pictures were taken after 6–8 h (exponential) and after 28 h (postdiauxic). Representative pictures are shown for each condition, showing (from left to right) bright field, green channel (GFP), red channel (mCherry), and the corresponding merged picture. (A) Colocalization with the ER. During exponential growth, nearly all cells displayed colocalization of Isc1-GFP with the ER-mCherry marker (plasmid FBp709). In postdiauxic-phase cells, two distinct populations are observed, showing either an overlap or no overlap with the ER. (B) Colocalization with mitochondria. During exponential growth, virtually no cells displayed colocalization of Isc1-GFP with the mitochondria-mCherry marker (plasmid FBp459). In postdiauxic phase cells, two distinct populations are observed, showing either an overlap or no overlap with the mitochondrial marker. For each condition, overlap was assessed in 100–150 cells of three independent transformants. Average results of overlap are noted with SDs, and unpaired *t* tests were performed to designate statistical difference of each type of colocalization between the WT strain and the *sch9Δ* strain at the postdiauxic phase (\**p* < 0.05, \*\*\**p* < 0.001).

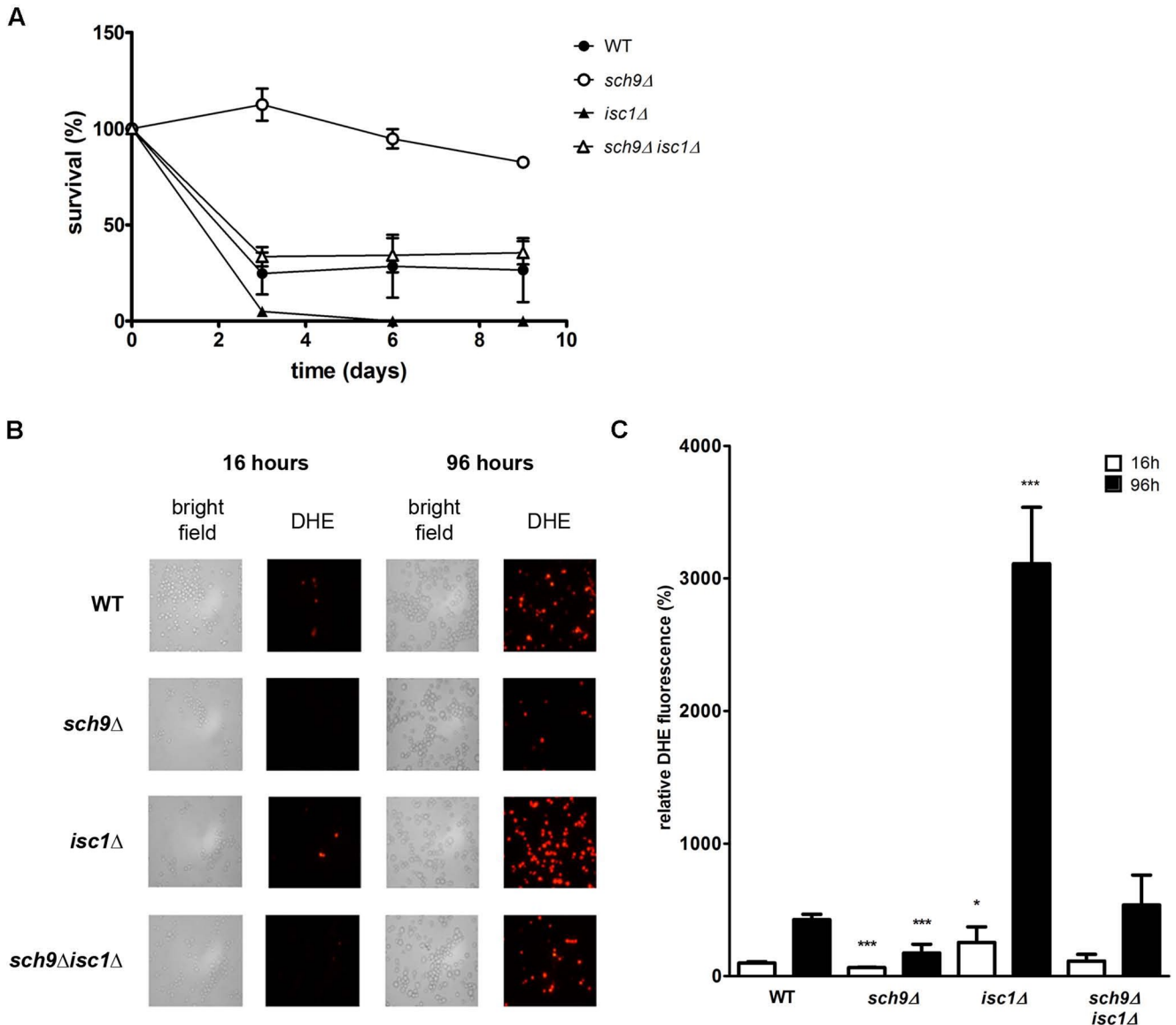


**FIGURE 9:** Control of viability and oxidative stress by *SCH9* and *ISC1* during chronological aging. (A) Chronological life span experiment. The viability of the wild-type (BY4741), *sch9Δ* (JW 01 306), *isc1Δ*, and *sch9Δisc1Δ* strains was measured by determining the colony-forming units (CFUs), expressed as percentage of CFUs observed at time 0 h. (B, C) The indicated strains were stained with dihydroethidium (DHE) for measurement of ROS accumulation after 16 h (exponential phase) and 96 h (stationary phase) of growth. (B) Fluorescence microscopic visualization of DHE-stained cells. (C) ROS levels quantified by fluorescence measurements (excitation, 535 nm; emission, 595 nm) and normalized for cell number. ROS levels of the WT strain at 16 h was set as 100%. Results in A and C are mean values of three independent cultures; error bars represent SD. In C, unpaired *t* tests were performed to designate statistical difference with ROS levels in the WT strain at the same time point (\**p* < 0.05, \*\*\**p* < 0.001).

1998). Yeast strains were grown at 30°C in YP (1% yeast extract, 2% bacto-peptone [OXOID, Aalst, Belgium]) or in synthetic growth medium (SG; 0.5% ammonium sulfate, 0.17% yeast nitrogen base without amino acids and without ammonium sulfate, and the appropriate synthetic drop-out amino acid/nucleotide mixture [ForMedium, Norfolk, UK]) supplemented with either 2% glucose (D) or 2% galactose (GAL) as indicated. Sporulation and tetrad analysis was carried out as described previously (Swinnen *et al.*, 2005).

#### Drug sensitivity assays

For analysis of sensitivity to myriocin and aureobasidin A, overnight yeast cultures in YPD were diluted to an OD<sub>600</sub> of 0.5 in YPD and further incubated at 30°C for 4–6 h. Sensitivity of the yeast cultures

to myriocin (Sigma-Aldrich, St. Louis, MO) was assayed by spotting 5-μl samples of 10-fold serial dilution of these yeast cultures on YPD plates containing 0.5 μg/ml myriocin. Growth was assessed after 48 h of incubation at 30°C. To determine sensitivity of the yeast cultures to aureobasidin A, 0.5 ml of these cultures was used to inoculate a YPD agar plate on which Whatman paper disks were placed containing 5 μl of 1 mg/ml aureobasidin A (Takara Bio, Shiga, Japan) in water. After 3 d of incubation at 30°C the size of the halo was measured. To assess sensitivity of yeast cultures to phytosphingosine (Sigma-Aldrich), cells were grown to stationary phase (>5 d) in YPD and subsequently diluted to an OD<sub>600</sub> of 0.05 in YPD containing 5 or 15 μM phytosphingosine and 0.0015% Nonidet P-40. The OD<sub>600</sub> of the different cultures was measured at regular time

points. For PI staining, yeast cells growing exponentially in YPD medium were treated for 2 h with 0.5 µg/ml myriocin. Next cells were collected, washed in phosphate-buffered saline, and stained with PI using the Annexin-V-Fluos Staining Kit (Roche Diagnostics, Vilvoorde, Belgium) according to the provided protocol.

### Northern blot analysis

Cells were grown to an OD<sub>600</sub> of 1.5 for a period of at least 24 h by repeated dilution. Samples were taken at the indicated time points, before and after the addition of 0.5 µg/ml myriocin. RNA extraction, probe preparation, and Northern blotting were performed as described previously (Swinnen *et al.*, 2005). Hybridized blots were exposed to phosphorimager screens, and images were scanned with a Bas 1000 PhosphorImager (Fujix, Tokyo, Japan).

### Sphingolipid analysis

Sphingolipid labeling and sphingolipidomics were performed as described previously (Kitagaki *et al.*, 2007; Thevissen *et al.*, 2010). In short, yeast cells growing exponentially in YPD medium were snap frozen in a methanol–dry ice bath and stored at –80°C. Electrospray tandem mass spectrometry (ESI-MS/MS) analysis of endogenous LCBs, their phosphates, and nonhydroxylated phytoceramide and dihydroceramide species was performed on a Thermo Finnigan TSQ 7000 triple quadrupole mass spectrometer (Thermo Scientific, Waltham, MA). Sphingolipid levels were expressed in pmol, normalized for the level of phospholipids (Pi, in nmol) present in the Bligh-Dyer lipid extract: pmol/nmol of Pi (Bligh and Dyer, 1959). For the analysis of complex inositolphosphoryl-containing sphingolipids, extracts were made from yeast cells grown to an OD<sub>600</sub> of 5 in YPD medium using a procedure described previously (Stock *et al.*, 2000). Sphingolipid analysis of the extracts was performed using ESI-MS on a Finnigan LCQ Deca mass spectrometer (Thermo Scientific) in the negative mode. Spectra were averaged over 100 scans. MS data were analyzed using Xcalibur software from Finnigan (Aerts *et al.*, 2006).

### Trichloroacetic acid protein extraction and Western blot

Samples for protein extraction were washed with 20% trichloroacetic acid (TCA) and stored at –80°C for extraction. Cells were resuspended in 20% TCA and broken with glass beads. Extracts were spun down at 4°C for 15 min at 13,000 rpm, and the pellet was washed twice with ice-cold acetone. Equal amounts of protein (Bradford quantification) were mixed with sample buffer and loaded onto an SDS-PAGE gel. Detection of the 9Myc-tagged proteins was performed with the anti-Myc antibody (BIOKE, Leiden, the Netherlands), and detection of internal Adh2 levels with the anti-Adh2 antibody (Millipore, Overijse, Belgium). Signals were quantified using UVP VisionWorks LS software (VWR, Leuven, Belgium).

### β-Galactosidase assay

Promoters of the *LAG1*, *LAC1*, *YDC1*, and *YPC1* genes were amplified using primers listed in Supplemental Table S3 and cloned into the *Bam*HI and *Sal*I sites of the multicopy lacZ reporter YEp357 (Serrano *et al.*, 2002), yielding plasmids FBp701–704. Subcloning of *SCH9* constructs was performed by cutting the *SCH9* coding regions from plasmids pJU675, pJU822, and pJU841 (Urban *et al.*, 2007) with *Xho*I and *Hind*III and ligating them into the pRS415 vectors, generating plasmids FBp705, FBp706, and FBp707. Precultures were grown overnight in SD-URA or SD-URA-LEU, inoculated into YPD medium, and grown for 6–7 h, after which part of the culture was treated with 200 nM rapamycin (Sigma-Aldrich). After 1 h, samples of treated and untreated cells were pelleted at 4°C and stored at –80°C. Cell pellets were resuspended in breaking buffer

(16.1 g of Na<sub>2</sub>HPO<sub>4</sub>·7H<sub>2</sub>O, 5.5 g of NaH<sub>2</sub>PO<sub>4</sub>·H<sub>2</sub>O, 0.75 g of KCl, 246 mg of MgSO<sub>4</sub>·7H<sub>2</sub>O per liter) containing proteinase inhibitor cocktail tablets (Complete Mini, EDTA free; Roche Diagnostics) and broken using glass beads. The clarified extract was diluted in breaking buffer to a total volume of 100 µl and incubated at 30°C for 5 min before the reaction was initiated by adding 20 µl of 4 mg/ml o-nitrophenylgalactoside (Sigma-Aldrich). At a precise time, the reaction was terminated by addition of 50 µl of 1 M Na<sub>2</sub>CO<sub>3</sub>. OD<sub>405nm</sub> was measured, and protein concentration was determined according to the Bradford method. We calculated specific activity from 1.7OD<sub>405nm</sub>/(0.0045 × protein concentration × extract volume × time), expressed as nmol/min mg protein. Data are the mean of three independent transformants. Error bars represent SD.

### Fluorescence microscopy

To study intracellular localization of Isc1, we received a construct expressing Isc1-GFP under the galactose-inducible promoter of the pYES2 vector (FBp431; Vaena de Avalos *et al.*, 2004). To study Isc1-GFP localization under conditions using glucose as a carbon source, we cloned *ISC1*-GFP behind its native promoter into plasmid pRS426 (2 µ, URA3). For this, we used plasmid FBp431 as a template for PCR of the *ISC1*-GFP fusion construct using primers *ISC1*-fus5 and *ISC1*-fus4. Yeast genomic DNA was used for PCR of the *ISC1* promoter using primers *ISC1*-fus1 and *ISC1*-RVC. Both PCR products contain overlapping ends with the pRS426 vector and each other, and a cotransformation of both PCR products with *Eco*RI-linearized pRS426 into yeast resulted in *in vivo* recombination to yield plasmid FBp708 (*p*<sub>*ISC1*</sub>*pr*-*ISC1*-GFPuv construct in pRS426). Correct cloning was confirmed by sequencing. Intracellular localization of Isc1-GFP was scored by assessing colocalization with mCherry markers for mitochondria (plasmid FBp459; mCherry targeted to the mitochondria by the Cox4 presequence) and the ER (plasmid FBp709). The latter plasmid was created in analogy with the strategy used by Okamoto *et al.* (2006). In short, an ER-targeted version of mCherry was made by fusing the Kar2p signal-peptide sequence (first 135 nucleotides) to the coding region of mCherry containing a C-terminal HDEL retention sequence. This was achieved by cotransformation of PCR products using primers KAR2-F1 and KAR2-F2 (genomic DNA template) and primers mCherry-F1 and mCherry-F2 (FBp459 template), with a *Bam*HI-linearized pYX242 plasmid. After recombination in yeast, plasmid FBp709 was formed, expressing the KAR2<sub>(1→135)</sub>-mCherry-HDEL fusion from the TPI promoter. Plasmids used are listed in Supplemental Table S2 and primers in Supplemental Table S3. Colocalization of Isc1-GFP (plasmid FBp431 or FBp708) with mCherry (plasmid FBp459 or FBp709) was carried out using a Leica DM 4000B fluorescence microscope (Leica Microsystems, Diegem, Belgium), and images were taken with a Leica DFC 420c camera using Leica Application software. Cultures were pregrown overnight on SG medium lacking uracil and leucine and transferred to YPGAL (FBp431) or YPD (FBp708) medium at an initial OD<sub>600</sub> of 0.5. Green and red fluorescence was monitored after 6–8 h (exponential phase) and after 28 h (postdiauxic phase).

### Chronological life span analysis and determination of ROS

For the analysis of chronological life span, cultures were pregrown in SG complete growth medium and diluted in flasks to an OD<sub>600</sub> of 0.1 in SG complete medium containing 2% glucose for 28 h, which was set as time zero for longevity assessment. At the indicated time points, cells were plated out on YPD agar plates, and colony-forming units were counted after 2 d of incubation at 30°C. For determination of ROS accumulation, cells were stained with dihydroethidium, pictures were taken with the fluorescence microscope, and

quantification was performed by fluorescence measurements (excitation, 535 nm; emission, 595 nm), normalized for cell number by measuring OD<sub>595</sub>, using a Beckman DTX880 plate reader (Molecular Devices, Wokingham, UK).

### Reproducibility of results

All experiments were performed at least three times with similar results. Where applicable, quantification was performed, and results are shown as mean values ± SD (shown as error bars). For other experiments, representative results are shown.

### ACKNOWLEDGMENTS

We thank R. Loewith for providing the plasmids encoding the *SCH9* constructs. Research was funded by grants of the Fonds Wetenschappelijk Onderzoek-Vlaanderen to J.W.; grants of KU Leuven to J.W., D.D.V., and B.C.; a Ph.D. grant of the Agency for Innovation by Science and Technology to P.D.S. and T.W.; and a postdoc grant of the Fonds Wetenschappelijk Onderzoek-Vlaanderen to E.S. K.T. acknowledges the receipt of a postdoctoral fellowship from the Industrial Research Fund, KU Leuven. This work was also partly supported by National Institutes of Health Grant GM63265; the Lipidomics Shared Resource, Hollings Cancer Center, Medical University of South Carolina (P30 CA138313); and the Lipidomics Core in the SC Lipidomics and Pathobiology COBRE, Department of Biochemistry, Medical University of South Carolina (NCRR Grant P20 RR017677).

### REFERENCES

Aerts AM, Francois IE, Bammens L, Cammue BP, Smets B, Winderickx J, Accardo S, De Vos DE, Thevissen K (2006). Level of M(IP)2C sphingolipid affects plant defensin sensitivity, oxidative stress resistance and chronological life-span in yeast. *FEBS Lett* 580, 1903–1907.

Almeida T et al. (2008). Isc1p plays a key role in hydrogen peroxide resistance and chronological lifespan through modulation of iron levels and apoptosis. *Mol Biol Cell* 19, 865–876.

Barbosa AD, Osorio H, Sims KJ, Almeida T, Alves M, Bielawski J, Amorim MA, Moradas-Ferreira P, Hannun YA, Costa V (2011). Role for Sit4p-dependent mitochondrial dysfunction in mediating the shortened chronological lifespan and oxidative stress sensitivity of Isc1p-deficient cells. *Mol Microbiol* 81, 515–527.

Bikman BT, Summers SA (2011). Ceramides as modulators of cellular and whole-body metabolism. *J Clin Invest* 121, 4222–4230.

Birbes H, El Bawab S, Hannun YA, Obeid LM (2001). Selective hydrolysis of a mitochondrial pool of sphingomyelin induces apoptosis. *FASEB J* 15, 2669–2679.

Bligh EG, Dyer WJ (1959). A rapid method of total lipid extraction and purification. *Can J Biochem Physiol* 37, 911–917.

Brachmann CB, Davies A, Cost GJ, Caputo E, Li J, Hieter P, Boeke JD (1998). Designer deletion strains derived from *Saccharomyces cerevisiae* S288C: a useful set of strains and plasmids for PCR-mediated gene disruption and other applications. *Yeast* 14, 115–132.

Breslow DK, Collins SR, Bodenmiller B, Aebersold R, Simons K, Shevchenko A, Ejsing CS, Weissman JS (2010). Orm family proteins mediate sphingolipid homeostasis. *Nature* 463, 1048–1053.

Breslow DK, Weissman JS (2010). Membranes in balance: mechanisms of sphingolipid homeostasis. *Mol Cell* 40, 267–279.

Carmona-Gutierrez D et al. (2011). Ceramide triggers metacaspase-independent mitochondrial cell death in yeast. *Cell Cycle* 10, 3973–3978.

Chipuk JE, McStay GP, Bharti A, Kuwana T, Clarke CJ, Siskind LJ, Obeid LM, Green DR (2012). Sphingolipid metabolism cooperates with BAK and BAX to promote the mitochondrial pathway of apoptosis. *Cell* 148, 988–1000.

Chung N, Mao C, Heitman J, Hannun YA, Obeid LM (2001). Phytosphingosine as a specific inhibitor of growth and nutrient import in *Saccharomyces cerevisiae*. *J Biol Chem* 276, 35614–35621.

Cowart LA, Shotwell M, Worley ML, Richards AJ, Montefusco DJ, Hannun YA, Lu X (2010). Revealing a signaling role of phytosphingosine-1-phosphate in yeast. *Mol Syst Biol* 6, 349.

Crauwels M, Donaton MC, Pernambuco MB, Winderickx J, de Winde JH, Thevelein JM (1997). The Sch9 protein kinase in the yeast *Saccharomyces cerevisiae* controls cAPK activity and is required for nitrogen activation of the fermentable-growth-medium-induced (FGM) pathway. *Microbiology* 143, 2627–2637.

Di Paola M, Cocco T, Lorusso M (2000). Ceramide interaction with the respiratory chain of heart mitochondria. *Biochemistry* 39, 6660–6668.

Dickson RC (2008). Thematic review series: sphingolipids. New insights into sphingolipid metabolism and function in budding yeast. *J Lipid Res* 49, 909–921.

Dickson RC (2010). Roles for sphingolipids in *Saccharomyces cerevisiae*. *Adv Exp Med Biol* 688, 217–231.

Dickson RC, Sumanasekera C, Lester RL (2006). Functions and metabolism of sphingolipids in *Saccharomyces cerevisiae*. *Prog Lipid Res* 45, 447–465.

Ella KM, Qi C, Dolan JW, Thompson RP, Meier KE (1997). Characterization of a sphingomyelinase activity in *Saccharomyces cerevisiae*. *Arch Biochem Biophys* 340, 101–110.

Fabrizio P, Pozza F, Pletcher SD, Gendron CM, Longo VD (2001). Regulation of longevity and stress resistance by Sch9 in yeast. *Science* 292, 288–290.

Funato K, Vallee B, Riezman H (2002). Biosynthesis and trafficking of sphingolipids in the yeast *Saccharomyces cerevisiae*. *Biochemistry* 41, 15105–15114.

Garcia-Ruiz C, Colell A, Mari M, Morales A, Fernandez-Checa JC (1997). Direct effect of ceramide on the mitochondrial electron transport chain leads to generation of reactive oxygen species. Role of mitochondrial glutathione. *J Biol Chem* 272, 11369–11377.

Gudz TI, Tserng KY, Hoppel CL (1997). Direct inhibition of mitochondrial respiratory chain complex III by cell-permeable ceramide. *J Biol Chem* 272, 24154–24158.

Hait NC, Oskeritzian CA, Paugh SW, Milstien S, Spiegel S (2006). Sphingosine kinases, sphingosine 1-phosphate, apoptosis and diseases. *Biochim Biophys Acta* 1758, 2016–2026.

Han S, Lone MA, Schneiter R, Chang A (2010). Orm1 and Orm2 are conserved endoplasmic reticulum membrane proteins regulating lipid homeostasis and protein quality control. *Proc Natl Acad Sci USA* 107, 5851–5856.

Hannun YA, Obeid LM (2011). Many ceramides. *J Biol Chem* 286, 27855–27862.

Heidler SA, Radding JA (1995). The AUR1 gene in *Saccharomyces cerevisiae* encodes dominant resistance to the antifungal agent aureobasidin A (LY295337). *Antimicrob Agents Chemother* 39, 2765–2769.

Huang X, Liu J, Dickson RC (2012). Down-regulating sphingolipid synthesis increases yeast lifespan. *PLoS Genet* 8, e1002493.

Kajiwara K, Muneoka T, Watanabe Y, Karashima T, Kitagaki H, Funato K (2012). Perturbation of sphingolipid metabolism induces endoplasmic reticulum stress-mediated mitochondrial apoptosis in budding yeast. *Mol Microbiol* 86, 1246–1261.

Kihara A, Mitsutake S, Mizutani Y, Igarashi Y (2007). Metabolism and biological functions of two phosphorylated sphingolipids, sphingosine 1-phosphate and ceramide 1-phosphate. *Prog Lipid Res* 46, 126–144.

Kim S, Fyrst H, Saba J (2000). Accumulation of phosphorylated sphingoid long chain bases results in cell growth inhibition in *Saccharomyces cerevisiae*. *Genetics* 156, 1519–1529.

Kitagaki H, Cowart LA, Matmati N, Montefusco D, Gandy J, de Avalos SV, Novgorodov SA, Zheng J, Obeid LM, Hannun YA (2009). ISC1-dependent metabolic adaptation reveals an indispensable role for mitochondria in induction of nuclear genes during the diauxic shift in *Saccharomyces cerevisiae*. *J Biol Chem* 284, 10818–10830.

Kitagaki H, Cowart LA, Matmati N, Vaena de Avalos S, Novgorodov SA, Zeidan YH, Bielawski J, Obeid LM, Hannun YA (2007). Isc1 regulates sphingolipid metabolism in yeast mitochondria. *Biochim Biophys Acta* 1768, 2849–2861.

Klose C, Surma MA, Gerl MJ, Meyenhofer F, Shevchenko A, Simons K (2012). Flexibility of a eukaryotic lipidome—insights from yeast lipidomics. *PLoS One* 7, e35063.

Kobayashi SD, Nagiec MM (2003). Ceramide/long-chain base phosphate rheostat in *Saccharomyces cerevisiae*: regulation of ceramide synthesis by Elo3p and Cka2p. *Eukaryot Cell* 2, 284–294.

Lavoie H, Whiteway M (2008). Increased respiration in the sch9Delta mutant is required for increasing chronological life span but not replicative life span. *Eukaryot Cell* 7, 1127–1135.

Lester RL, Withers BR, Schultz MA, Dickson RC (2013). Iron, glucose and intrinsic factors alter sphingolipid composition as yeast cells enter stationary phase. *Biochim Biophys Acta* 1831, 726–736.

- Levade T, Malagarie-Cazenave S, Gouaze V, Segui B, Tardy C, Betito S, Andrieu-Abadie N, Cuvillier O (2002). Ceramide in apoptosis: a revisited role. *Neurochem Res* 27, 601–607.
- Liu J, Huang X, Withers BR, Blalock E, Liu K, Dickson RC (2013). Reducing sphingolipid synthesis orchestrates global changes to extend yeast lifespan. *Aging Cell* 12, 833–841.
- Liu K, Zhang X, Lester RL, Dickson RC (2005). The sphingoid long chain base phytosphingosine activates AGC-type protein kinases in *Saccharomyces cerevisiae* including Ypk1, Ypk2, and Sch9. *J Biol Chem* 280, 22679–22687.
- Liu M, Huang C, Polu SR, Schneider R, Chang A (2012). Regulation of sphingolipid synthesis through Orm1 and Orm2 in yeast. *J Cell Sci* 125, 2428–2435.
- Matmati N, Hannun YA (2008). Thematic review series: sphingolipids. ISC1 (inositol phosphosphingolipid-phospholipase C), the yeast homologue of neutral sphingomyelinases. *J Lipid Res* 49, 922–928.
- Matmati N, Metelli A, Tripathi K, Yan S, Mohanty BK, Hannun YA (2013). Identification of C18:1-phytoceramide as the candidate lipid mediator for hydroxyurea resistance in yeast. *J Biol Chem* 288, 17272–17284.
- McCourt PC, Morgan JM, Nickels JT Jr (2009). Stress-induced ceramide-activated protein phosphatase can compensate for loss of amphiphysin-like activity in *Saccharomyces cerevisiae* and functions to reinitiate endocytosis. *J Biol Chem* 284, 11930–11941.
- Miyake Y, Kozutsumi Y, Nakamura S, Fujita T, Kawasaki T (1995). Serine palmitoyltransferase is the primary target of a sphingosine-like immunosuppressant, ISP-1/myriocin. *Biochem Biophys Res Commun* 211, 396–403.
- Nagiec MM, Nagiec EE, Baltisberger JA, Wells GB, Lester RL, Dickson RC (1997). Sphingolipid synthesis as a target for antifungal drugs. Complementation of the inositol phosphorylceramide synthase defect in a mutant strain of *Saccharomyces cerevisiae* by the AUR1 gene. *J Biol Chem* 272, 9809–9817.
- Nickels JT, Broach JR (1996). A ceramide-activated protein phosphatase mediates ceramide-induced G1 arrest of *Saccharomyces cerevisiae*. *Genes Dev* 10, 382–394.
- Okamoto M, Yoko-o T, Umemura M, Nakayama K, Jigami Y (2006). Glycosylphosphatidylinositol-anchored proteins are required for the transport of detergent-resistant microdomain-associated membrane proteins Tat2p and Fur4p. *J Biol Chem* 281, 4013–4023.
- Olivera A, Kohama T, Edsall L, Nava V, Cuvillier O, Poulton S, Spiegel S (1999). Sphingosine kinase expression increases intracellular sphingosine-1-phosphate and promotes cell growth and survival. *J Cell Biol* 147, 545–558.
- Pan Y, Schroeder EA, Ocampo A, Barrientos A, Shadel GS (2011). Regulation of yeast chronological life span by TORC1 via adaptive mitochondrial ROS signaling. *Cell Metab* 13, 668–678.
- Pan Y, Shadel GS (2009). Extension of chronological life span by reduced TOR signaling requires down-regulation of Sch9p and involves increased mitochondrial OXPHOS complex density. *Aging (Albany NY)* 1, 131–145.
- Pascual-Ahuir A, Proft M (2007). Control of stress-regulated gene expression and longevity by the Sch9 protein kinase. *Cell Cycle* 6, 2445–2447.
- Pedruzzi I, Dubouloz F, Cameroni E, Wanke V, Roosen J, Winderickx J, De Virgilio C (2003). TOR and PKA signaling pathways converge on the protein kinase Rim15 to control entry into G0. *Mol Cell* 12, 1607–1613.
- Rego A, Costa M, Chaves SR, Matmati N, Pereira H, Sousa MJ, Moradas-Ferreira P, Hannun YA, Costa V, Corte-Real M (2012). Modulation of mitochondrial outer membrane permeabilization and apoptosis by ceramide metabolism. *PLoS One* 7, e48571.
- Roelants FM, Breslow DK, Muir A, Weissman JS, Thorne J (2011). Protein kinase Ypk1 phosphorylates regulatory proteins Orm1 and Orm2 to control sphingolipid homeostasis in *Saccharomyces cerevisiae*. *Proc Natl Acad Sci USA* 108, 19222–19227.
- Roelants FM, Torrance PD, Thorne J (2004). Differential roles of PDK1- and PDK2-phosphorylation sites in the yeast AGC kinases Ypk1, Pkc1 and Sch9. *Microbiology* 150, 3289–3304.
- Roosen J, Engelen K, Marchal K, Mathys J, Griffioen G, Cameroni E, Thevelein JM, De Virgilio C, De Moor B, Winderickx J (2005). PKA and Sch9 control a molecular switch important for the proper adaptation to nutrient availability. *Mol Microbiol* 55, 862–880.
- Saddoughi SA, Song P, Ogetmen B (2008). Roles of bioactive sphingolipids in cancer biology and therapeutics. *Subcell Biochem* 49, 413–440.
- Sawai H, Okamoto Y, Luberto C, Mao C, Bielawska A, Domae N, Hannun YA (2000). Identification of ISC1 (YER019w) as inositol phosphosphingolipid phospholipase C in *Saccharomyces cerevisiae*. *J Biol Chem* 275, 39793–39798.
- Serrano R, Ruiz A, Bernal D, Chambers JR, Arino J (2002). The transcriptional response to alkaline pH in *Saccharomyces cerevisiae*: evidence for calcium-mediated signalling. *Mol Microbiol* 46, 1319–1333.
- Shimobayashi M, Oppliger W, Moes S, Jenö P, Hall MN (2013). TORC1-regulated protein kinase Npr1 phosphorylates Orm to stimulate complex sphingolipid synthesis. *Mol Biol Cell* 24, 870–881.
- Sims KJ, Spassieva SD, Voit EO, Obeid LM (2004). Yeast sphingolipid metabolism: clues and connections. *Biochem Cell Biol* 82, 45–61.
- Siskind LJ (2005). Mitochondrial ceramide and the induction of apoptosis. *J Bioenerg Biomembr* 37, 143–153.
- Siskind LJ, Kolesnick RN, Colombini M (2002). Ceramide channels increase the permeability of the mitochondrial outer membrane to small proteins. *J Biol Chem* 277, 26796–26803.
- Skrzypek MS, Nagiec MM, Lester RL, Dickson RC (1998). Inhibition of amino acid transport by sphingoid long chain bases in *Saccharomyces cerevisiae*. *J Biol Chem* 273, 2829–2834.
- Smets B, De Snijder P, Engelen K, Joossens E, Ghillebert R, Thevissen K, Marchal K, Winderickx J (2008). Genome-wide expression analysis reveals TORC1-dependent and -independent functions of Sch9. *FEMS Yeast Res* 8, 1276–1288.
- Smets B, Ghillebert R, De Snijder P, Binda M, Swinnen E, De Virgilio C, Winderickx J (2010). Life in the midst of scarcity: adaptations to nutrient availability in *Saccharomyces cerevisiae*. *Curr Genet* 56, 1–32.
- Stock SD, Hama H, Radding JA, Young DA, Takemoto JY (2000). Syringomycin E inhibition of *Saccharomyces cerevisiae*: requirement for biosynthesis of sphingolipids with very-long-chain fatty acids and mannose- and phosphoinositol-containing head groups. *Antimicrob Agents Chemother* 44, 1174–1180.
- Sun Y, Miao Y, Yamane Y, Zhang C, Shokat KM, Takematsu H, Kozutsumi Y, Drubin DG (2012). Orm protein phosphoregulation mediates transient sphingolipid biosynthesis response to heat stress via the Pkh-Ypk and Cdc55-PP2A pathways. *Mol Biol Cell* 23, 2388–2398.
- Sun Y, Taniguchi R, Tanoue D, Yamaji T, Takematsu H, Mori K, Fujita T, Kawasaki T, Kozutsumi Y (2000). Slit2 (Ypk1), a homologue of mammalian protein kinase SGK, is a downstream kinase in the sphingolipid-mediated signaling pathway of yeast. *Mol Cell Biol* 20, 4411–4419.
- Swinnen E, Rosseels J, Winderickx J (2005). The minimum domain of Pho81 is not sufficient to control the Pho85-Rim15 effector branch involved in phosphate starvation-induced stress responses. *Curr Genet* 48, 18–33.
- Thevissen K, Yen WL, Carmona-Gutierrez D, Idkowiak-Baldys J, Aerts AM, Francois IE, Madeo F, Klionsky DJ, Hannun YA, Cammue BP (2010). Skn1 and Ipt1 negatively regulate autophagy in *Saccharomyces cerevisiae*. *FEMS Microbiol Lett* 303, 163–168.
- Toda T, Cameron S, Sass P, Wigler M (1988). SCH9, a gene of *Saccharomyces cerevisiae* that encodes a protein distinct from, but functionally and structurally related to, cAMP-dependent protein kinase catalytic subunits. *Genes Dev* 2, 517–527.
- Urban J *et al.* (2007). Sch9 is a major target of TORC1 in *Saccharomyces cerevisiae*. *Mol Cell* 26, 663–674.
- Vaena de Avalos S, Okamoto Y, Hannun YA (2004). Activation and localization of inositol phosphosphingolipid phospholipase C, Isc1p, to the mitochondria during growth of *Saccharomyces cerevisiae*. *J Biol Chem* 279, 11537–11545.
- Vaena de Avalos S, Su X, Zhang M, Okamoto Y, Dowhan W, Hannun YA (2005). The phosphatidylglycerol/cardiolipin biosynthetic pathway is required for the activation of inositol phosphosphingolipid phospholipase C, Isc1p, during growth of *Saccharomyces cerevisiae*. *J Biol Chem* 280, 7170–7177.
- Van Brocklyn JR, Williams JB (2012). The control of the balance between ceramide and sphingosine-1-phosphate by sphingosine kinase: oxidative stress and the seesaw of cell survival and death. *Comp Biochem Physiol B Biochem Mol Biol* 163, 26–36.
- Voordeckers K, Kimpe M, Haesendonckx S, Louwet W, Versele M, Thevelein JM (2011). Yeast 3-phosphoinositide-dependent protein kinase-1 (PDK1) orthologs Pkh1–3 differentially regulate phosphorylation of protein kinase A (PKA) and the protein kinase B (PKB)/S6K ortholog Sch9. *J Biol Chem* 286, 22017–22027.
- Wei M, Fabrizio P, Madia F, Hu J, Ge H, Li LM, Longo VD (2009). Tor1/Sch9-regulated carbon source substitution is as effective as calorie restriction in life span extension. *PLoS Genet* 5, e1000467.
- Yorimitsu T, Zaman S, Broach JR, Klionsky DJ (2007). Protein kinase A and Sch9 cooperatively regulate induction of autophagy in *Saccharomyces cerevisiae*. *Mol Biol Cell* 18, 4180–4189.